IMPACT OF ELECTRIC VEHICLE ON SMART GRID

A DISSERTATION

Submitted in partial fulfilment of the
Requirement for the award of degree
Of
MASTER OF TECHNOLOGY
In
ELECTRICAL ENGINEERING
(With specialization in Power System Engineering)

By

PRASANTA KUMAR MOHANTY
(17529009)

DEPARTMENT OF ELECTRICAL ENGINEERING
INDIAN INSTITUTE OF TECHNOLOGY ROORKEE
ROORKEE- 247667 (INDIA)

MAY, 2019

CANDIDATE'S DECLARATION

I hereby declare that the dissertation entitled " **Impact of Electric Vehicle On Smart Grid"**, submitted to the Department of Electrical Engineering, Indian Institute of Technology, Roorkee, India, in partial fulfilment of the requirements for the award of the degree of **Master of Technology in Electrical Engineering** with specialization in Power Systems engineering is an authentic record of the work carried out by me during the period from June 2018 to May 2019 under the supervision of **Dr. Premalata Jena,** Assistant Professor, Department of Electrical Engineering, Indian Institute of Technology, Roorkee. The matter presented in this dissertation report has not been submitted by me for the award of any other degree of this institute or any other institute.

<div align="right">

(PRASANTA KUMAT MOHANTY)

</div>

Date: Enrolment Number: 17529009

Place: Roorkee   Power Systems Engineering

CERTIFICATE

This is to certify that the above statement made by the candidate is true to the best of my knowledge and belief.

Date: Dr. Premalat Jena

Place: Roorkee   Assistant Professor

                                                                         Department of Electrical Engineering

                                                                         Indian Institute of Technology, Roorkee

                                                                         Roorkee-247667, Uttarakhand, India

ACKNOWLEDGEMENT

I take this opportunity to express my heartiest gratitude to all those who have lent their help and contribution in various forms to complete this project successfully. I am highly indebted to my supervisor **Dr. Premalata Jena,** Assistant Professor, Department of Electrical Engineering, Indian Institute of Technology, Roorkee, my mentor and guide who has been a constant source of inspiration and knowledge to complete my project. Her keen interest and constant encouragement gave me the confidence to complete my work. I specially thank all the faculty members of Power Systems Engineering, who have contributed, with their encouraging words, constructive criticism and valuable suggestions, in a significant way towards the completion of this dissertation.

I would like to thank my parents, God and my friends who in any manner have supported and helped me during the course of this project.

<div align="right">

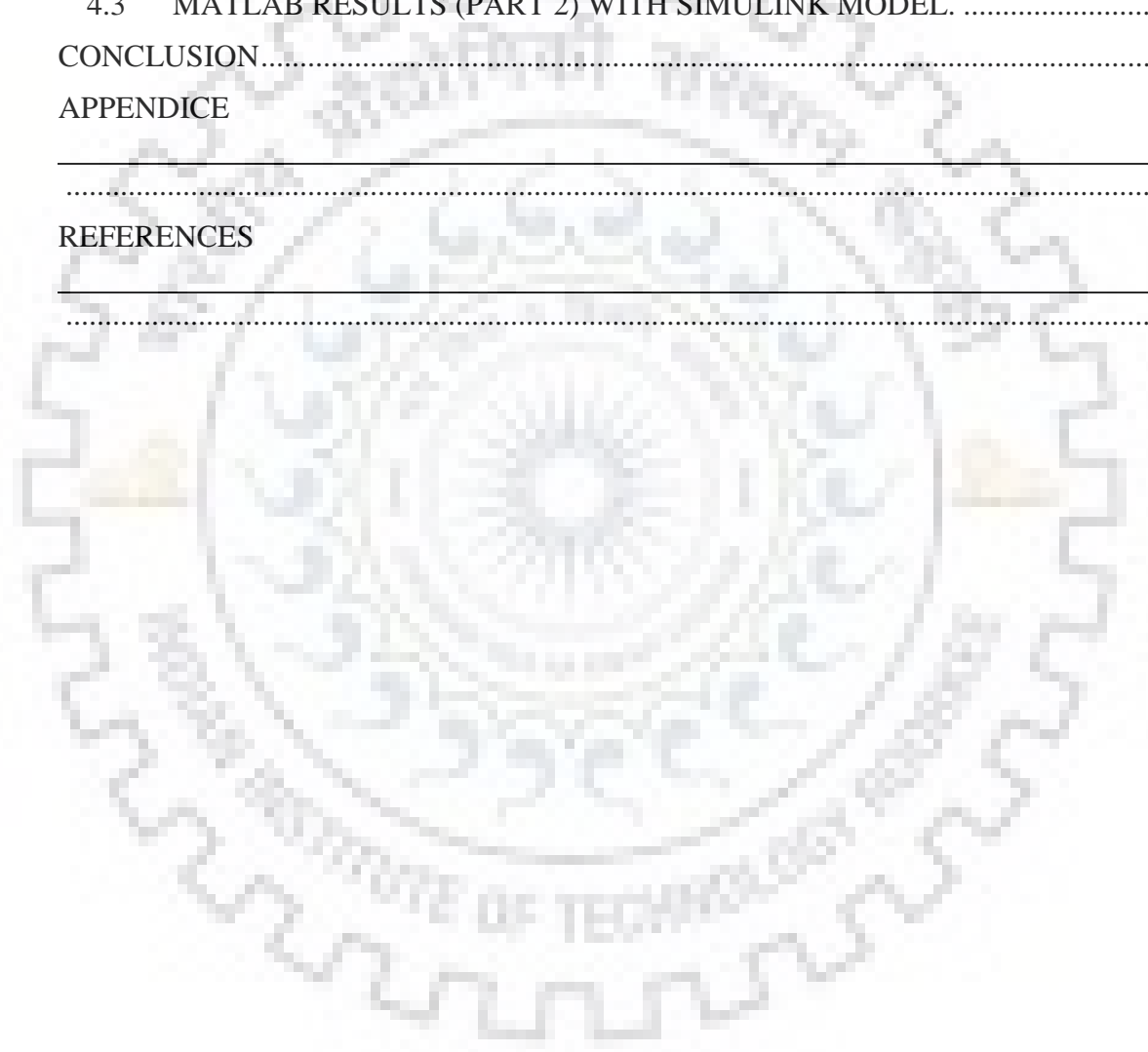**PRASANTA KUMAR MOHANTY**

</div>

ABSTRACT

Alternative vehicles, such as plug-in hybrid electric vehicles, are becoming more popular. The batteries of these plug-in hybrid electric vehicles are to be charged at home from a standard outlet or on a corporate car park. These extra electrical loads have an impact on the distribution grid like power quality issues, voltage deviation and power loss. First of all a bidirectional electric vehicle battery charger which operates in all four quadrants of P-Q (Active-Reactive) plane. The charger is composed of full bridge AC-DC converter and bi-directional DC-DC converter to operate in G2V mode. Secondly a solar PV (Photo-voltaic) array based EV (Electric Vehicle) charger is presented, which has a bidirectional flow of active and reactive powers. The proposed charger uses a solar PV array energy to charge the EV battery and to feed the grid with the remaining power. In this charger, the VSC (Voltage Source Converter) does the task of harnessing the maximum power from the solar PV array. At the time of high cost of energy, the charger has the provision to inject the battery energy into the grid to earn revenue. In addition to the active power exchange with the grid, the proposed charger also exchanges the reactive power with the grid, simultaneously. In all operating modes, the THD (Total Harmonic Distortion) of the grid current remains within the IEEE 519 standard. The proposed charger is designed for a single phase 230V, 50Hz supply.

CONTENTS

LIST OF FIGURES

LIST OF ABBREVATIONS

PCC   Point of Common Coupling

PLL   Phase Locked Loop

PI   Proportional Integrator

DG   Distributed Generation

DER   Distributed Energy Resource

G2V   Grid to vehicle

V2G   Vehicle to Grid

BEV   Battery only Vehicle

SOC   State of charge

P   Active power

Q   Reactive power

k_p Proportional controller gain

k_i Integral controller gain

IGBT   insulated Gate Bipolar Transistor

Chapter 1
INTRODUCTION

1.1 OVERVIEW

The International panel on climate change (IPCC) releases a report on climate change which concludes that the increase in average temperatures at the global level since the past few decades is mainly due to the increase in Green House Gases (GHG) concentrations. EU reduction targets reduction of GHG emissions by 25% till 2020 compared to 1990 and at least 15% renewable energy in the transport sector.

The history of electric vehicle starts in 1868. Since then, studies were going on in utilizing EV as future Vehicle. EV charging station is the place where an EV integrates with the distribution grid. So, expert care has to be given in designing the components in the charging station to ensure a quality grid integration. Also, since the EV has to be user friendly, we have to reduce the charging time. Therefore, the work has been done for a Level 3(200/600V DC, up to 240kW, 400A) EV charging outlet which ensures fast DC charging. The integration of EV the grid offers a lot of challenges in power quality. The design of different elements in the proposed model is precisely done to aid quality power exchange. The AC-DC converter employs a control in dq reference frame. The DC-DC converter which aids the EV battery charging/discharging employs constant voltage/ constant current strategy. The control strategies tries to fulfil recent IEEE standards 14592010 with the objective of maximizing the use/injection of AC power from/into the grid reducing the lower order harmonic factor. In the proposed paper, different aspects of EV integration to grid are analysed and the results are shown.

Electric Vehicles forming a major proportion of transport sector have the potential to reduce these emissions due to higher efficiencies along with the possibility to be powered by renewable energy. EV not only utilizes renewable power, but also facilitates higher shares of power generation because the batteries of vehicle fleet can act as power storage. Also electricity can be produced from many different energy sources, making it possible to reduce the dependency on fossil fuels of the transport factor.

EVs are gaining popularity these days as demonstrated by the various vehicles made available in the market by almost all automobile companies. The main energy storage systems of these vehicles are the electrochemical batteries which impose a limit on driving distances, hence different models of EV can have different range depending upon their battery capacity and charging methods.

1.2 PROBLEM STATEMENT

This report presents a smart compactible integration of EV with the distribution grid assuring a quality power. In this report, works have been done on charging of electric vehicle from a one phase ac outlet that can charge EV, which will alleviate the down-time required for vehicle charging. There is a master control to deal with the power exchange between the AC and DC bus (AC-DC Converter Control).The control of individual EV is de-centralized (DC-DC Converter Control). The proposed work looks into aspect of EV integration to grid like grid to vehicle modeG2V (EV charging). This report wants to emphasize on implementation of solar PV array based multifunctional EV charger. In all the described modes, the THD (total harmonic distortion) of the grid current remains within the IEEE 519 standard. It also eliminate the need of DC-DC boost converter. Simulation platform is Matlab.

1.3 LITERATURE REVIEW

In [1],the modelling of bi-directional converter with front end AC-DC PFC converter and reversible DC-DC converter is given. [2] have proposed an electric vehicle charger that has a capability of operating in Four quadrant PQ(Active-Reactive) plane. In the current scenario, the electric vehicle is emerging as a promising solution to the problems caused by the fossil fuel powered vehicles [3]. [4] have proposed to provide the reactive power support to the grid using the voltage source converter (VSC). Nowadays most of the loads are nonlinear, and they draw non-sinusoidal current from the grid. Because of this, the harmonics are injected into the grid. The advantage of this kind of charging station is that the solar PV power is generated locally and used locally [5]. Because of this, the transmission lines need not to be upgraded for the high power.

A survey suggest that the adaptability of the battery operated vehicle is expected to increase exponentially and to comprise of 23-25% of the market by 2030 in USA. Nevertheless, with the rapid increase of battery operated vehicles a large amount of energy is expected to be stored in the battery, creating a scope of power flow in contrary direction (Battery to grid). This gives rise to

bidirectional on-board and off-board chargers, enabled with the power flow in contrary direction from battery to the grid [6],[7].

The purpose of the VSC control is to regulate the DC bus voltage and control the grid current for controlling the active and reactive power flow, thereby generating the switching pulses for the VSC. The DC bus voltage regulation is achieved by a proportional integral (PI) controller[8] used for minimizing the error between actual DC bus voltage (Vdc) and reference DC bus voltage (Vdc*). [9] have utilized the V2G functionality of the EV charger for improving the power quality of the grid. [10] have proposed the implementation of the solar PV based charging station. [11] have proposed the solar PV array and wind energy based grid connected system. However, this requires the revamping of the transmission lines for carrying more power. It also incurs transmission power losses. However, the adaptability of EV (Electric Vehicle) in society, depends on the charging infrastructure[12]

1.4 PEV TECHNOLOGY

1.4.1 OVERVIEW

A plug-in electric vehicle uses electric energy from the battery as its primary energy source. The use of battery in PEV reduces or even eliminates the need for any kind of fuel. The vehicles have batteries to supply the required energy and these will need to plug into recharge. These electric vehicles were first urbanized in 1830s by a number of inventors.

1.4.2 ADVANTAGES OF PEV TECHNOLOGY

The PEV technology has been found suitable and is promoted in various countries for its positive ecological impacts and climatic change challenges. Adoption of PEV has the following benefits:

- **Energy security:** Electricity is derived from household resources, while sinking petroleum imports resulting into nation's energy autonomy. PEVs can contribute effectively to a unbiased assortment of domestically produced electrical energy.
- **Cleaner Environment:** Being environment friendly PEVs are effective in reducing total GHG emissions. The continuing tendency of increased electricity generation from renewable sources promises remuneration of reduced emissions.
- **Beneficial for economy:** PEVs have positive impacts on the local and as well as on national economies by creating new job opportunities in countries manufacturing PEV. Use of PEVs

eliminates the fuel cost that produces less expensive transportation. PEV charging stations can be located at businesses, retail stores, colleges, workplaces, parks and libraries.

- **Vehicle to grid:** Taking energy from the grid when required and selling back electrical energy to the grid provided a market scenario for the owner.

Battery can be charged when prices are low while the same can be discharged when electricity prices rise, thereby making the profit.

1.4.3 DIFFERENT TYPES OF ELECTRIC VEHICLES

Mainly there are four types of electric vehicles:

1. **Hybrid electric vehicles (HEVs):** The HEV uses a tiny battery to complement an interior ignition engine, it is re-energized by gasoline engine and regenerative braking.
2. **Plug-in hybrid electric vehicles (PHEVs):** PHEVs are driven by both electric motor and the interior ignition engine. We can charge them directly from the grid and also they have large battery capacity.
3. **Extended range electric vehicles (EREVs):** In EREV an electric generator is powered by interior ignition engine which is then used to charge the battery of the system. Unlike HEVs and PHEVs, wheels of the EREVs are driven by electric motor. The interior ignition engine only charges the battery.
4. **Battery electric vehicles (BEVs):** It does possess any interior ignition engine. It is charged directly from the grid. These types of vehicles have larger size of the battery as compared to any other type of electric vehicle.

1.4.4 PEV SYSTEMS

PEVs use only electricity to propel them rather than any other kind of fuel or ignition engine. Various parts of PEV system are given below:

- **Electric Motors:** It transforms electrical energy which is stored in the battery to mechanical energy, hence it makes the vehicle move forward or backward by AC or DC motor.

- **Electric Generators:** The generator is used to convert mechanical energy into electrical energy. These generators are driven by internal combustion engine in some electric vehicles.

- **Inverters:** The inverter converts DC power stored in the battery into AC and powers the AC motor where AC motor is used to drive the vehicle.

• **Chargers:** They are used to convert AC taken from the grid into DC power, which can be then stored in the batteries of electric vehicles. They consist of a control mechanism that optimizes the charging process that also extends the life of the battery.

• **Battery packs:** Electrical energy is stored in the batteries pack which is then used to power a PEV using a motor. Different EV uses different types of battery packs- lead acid, NiMH, Li-ion out of which Li-ion battery pack is more common. Battery packs attribute heavily to the significant price difference between normal vehicles and PEVs.

Chapter 2

BI-DIRECTIONAL CHARGER FOR ELECTRIC VEHICLE WITH FOUR QUADRANT CAPABILITIES

2.1 CONFIGURATION OF PROPOSED SYSTEM

Fig.2.1 shows the circuit topology of proposed charger. In this proposed charger two converters shares a common DC link. One converter interface with the grid and other with the battery. The grid side converter is a bi-directional AC-DC converter operating in power factor correction (PFC) mode and it make sure that power drawn from grid is a unity power factor. During G2V mode, this converter as shown in Fig.2.1, operates as a rectifier transforming power to the battery through the DC link capacitor.
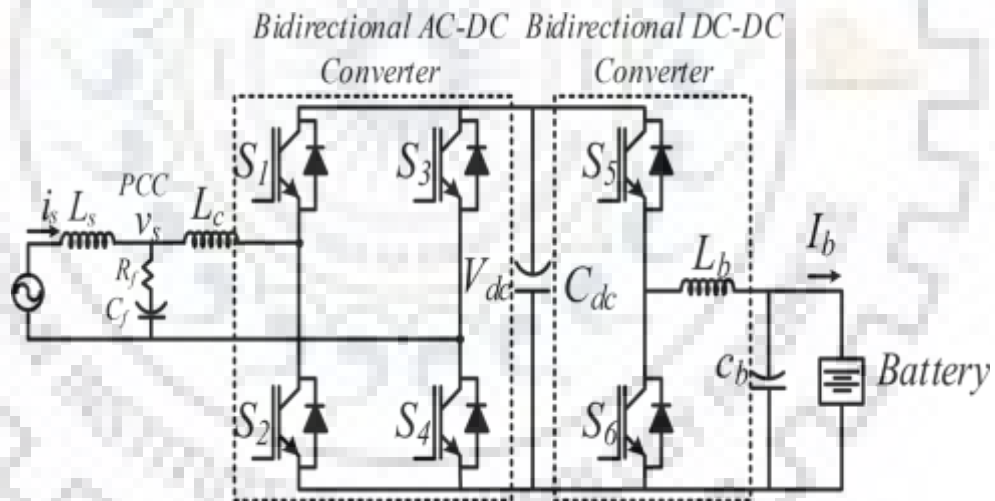

Fig.2. 1 circuit topology of Bi-directional battery charger

In case of reactive power compensation, the power drawn and fed to the grid is not to be at unity power factor and power factor depends on the amount of reactive power exchange. An interfacing of the battery requires a bidirectional DC-DC converter. During G2V mode, it act as a buck converter to control the charging voltage and current. The charging of the battery is achieved in two stage. The constant current charging is achieved to charge the battery for less than the specified voltage and once specified limit is reached the charging switches to voltage charging mode.

6

In this charger, the constant current charging is conducted to charge the battery. It is also support the reactive power demand to the grid. As per the agreement between grid and user, the converter operates to compensate the reactive power demand in both G2V and V2G modes. The converter support the four quadrant operation i.e. it charges or discharges the battery and injects into or absorbs the reactive power from the grid. The complete system diagram and quadrant operation in P-Q power plane are shown in Fig.2.2.
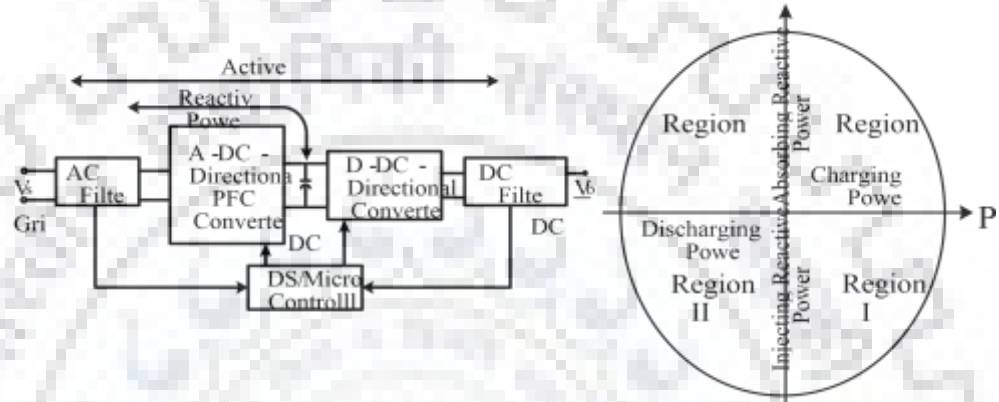

Fig.2. 2 Complete system diagram and quadrant operation in P-Q power plane

2.2   DESIGN OF PROPOSED SYSTEM

The front end of AC-DC converter is designed for 5 kW. The minimum DC link voltage is required for power transfer. So 400V is considered for design of DC link capacitor. DC link capacitor is designed for second harmonics of fundamental frequency and is given as

$$C_{dc}=\frac{I_{dc}}{2*w*\Delta V_{dc}}=\frac{P_{dc}/V_{dc}}{2*w*\Delta V_{dc}}=\frac{3000/400}{2*314*0.015*400}=1990.4\mu F \qquad (2.1)$$

The selected value of DC link capacitor for simulation is 2000μF. The design of interfacing inductor is designed for 20 kHz and peak of fundamental supply current of 20A. The current ripple is taken as 3% of the fundamental supply current.

$$L_c=\frac{m*V_{dc}}{6*f_{s*h}*\Delta I_c}=\frac{400}{6*20*10^3*1.2*20*.03}=4.62mH \qquad (2.2)$$

Hence 5mH is selected for simulation.

7

To prevent the injection of high frequency switching harmonics into the supply system, an inductive capacitive low pass filter is designed whose maximum value, C_{max} is calculated as

$$C_{max} = \frac{I_{peak}}{w_L * V_{peak}} \tan(\Theta) = \frac{20 * \sqrt{2}/230}{314 * 230 * \sqrt{2}} \tan(1°) = 318nF \tag{2.3}$$

Where V_{peak} and I_{peak} are amplitude of supply current and voltage and Θ is the displacement angle between them. Hence, the filter capacitor of 330nF is selected.

Now, the value of filter inductor is selected for considering the source inductance (Ls) of 4-5% of the source inductance. Hence, the total inductance is given as

$$L_a = \frac{1}{4 * \pi^2 * f_c^2 * C_{ac}} = \frac{1}{4 * \pi^2 * 4000^2 * 330 * 10^{-9}} = 19.19 \text{mH} \tag{2.4}$$

$L_a = 20 \text{mH}$

Where, f_c is the cut off frequency of the filter and is selected as 4000Hz.

The DC-DC converter is designed as buck converter and the DC side filter inductor is designed as

$$L_f = \frac{V_{dc} * k * (k-1)}{f * \Delta I_b} = \frac{400 * 0.75 * 0.25}{32 * 1000 * 10 * .05} = 4.68 \text{mH} \tag{2.5}$$

Where, V_{dc} is DC link voltage, f is switching frequency and k is the duty ratio of the buck converter. Hence 5mH is selected as filter inductor value and the DC side filter capacitor of 700μF is selected.

2.3 CONTROLLER DESIGN FOR G2V MODE

The controller for bi-directional charger is designed keeping four quadrants operation in PQ plane with the centre i.e. Active and reactive powers flow from and to the grid. The active power from the grid to the battery is considered positive and from the battery to the grid is taken negative. The reactive power from the grid is considered positive and in the quadrant diagram it is termed as an absorption of the reactive power. The reactive power of the grid is termed as negative. The control of the converter shown in Fig.2.1, which is designed in two stages, (1) AC-DC converter control, and (2) DC-DC converter. The control of AC-DC converter is achieved by estimating the active and reactive powers and commanded power at PCC as shown in Fig.2.The power at PCC is estimated by applying pq theory of three phase system, same theory is applied by assigning $V_\alpha = V_s, i_\alpha = i_s$. where

8

and are sensed voltage and current signals at PCC. The quadrature components of pq theory are obtained by delaying the sensed signals by quadrature cycle. Therefore, active and reactive power are estimated as,

$$p = \frac{1}{2}(V_\alpha * i_\alpha + V_\beta * i_\beta) = P_{ac} + P_{dc} \tag{2.6}$$

$$q = \frac{1}{2}(V_\alpha * i_\beta + V_\beta * i_\alpha) = Q_{ac} + Q_{dc} \tag{2.7}$$

Moreover, two low pass filters are used for both the outputs to obtained fundamental active and reactive powers (Pdc and Qdc). The AC-Dc converter control is designed to track the active and reactive powers demand at PCC. The active and reactive powers commands at PCC are decided by agreement between utility and the user. During peak hours, the utility pus the command for an active power. However the user has the freedom to choose whether to discharge or not. Similarly reactive power demand also decided. In return the utility must give some benefits to users for coordinated charging and discharging. The control loop design for AC-DC converter requires the phase angle of sensed supply voltage for generating the reference current signal. Single phase locked loop (PLL) is used for tracking the phase angle of the supply voltage. Single phase PLL utilises sensed supply voltage and its quadrature signal in α-β coordinates.

Fig.2.3 shows the control diagram for the G2V mode. For G2V mode, the active power flow from grid to vehicle and the active power demand (P_{cmd}) is given by the user. Therefore, the commanded amount of power must reach the battery.

Therefore the current reference for the DC-DC converter is generated by the division of P_{cmd} and the battery voltage V_b as,

$$I_b^* = \frac{P_{cmd}}{V_b} \tag{2.8}$$

This reference battery current I_b^* and the sensed battery current I_b , are processed through the hysteresis current controller for generating the gating pulses for the DC-DC converter.

An AC-DC converter current reference is generated by separately calculating the active and reactive components of the current reference. The active component I_{active} is sum of the battery current for delivering commanded amount of power and the loss component (I_{dc}) for maintaining DC link capacitor voltage to V_{dc}.
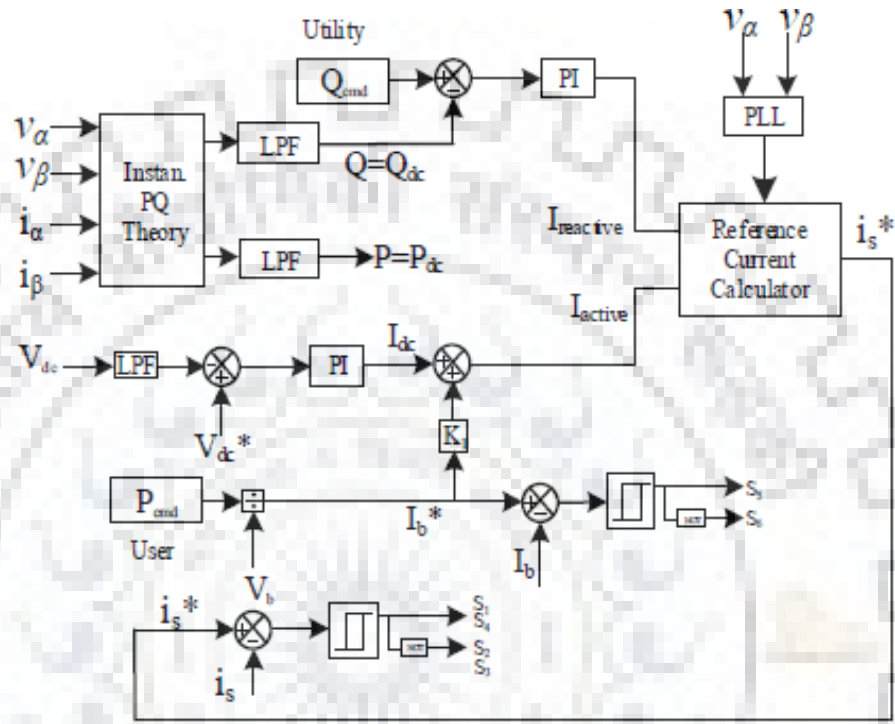
9

Fig.2. 3 Control diagram for G2V mode

The reference DC link voltage (V_{dc}^*) is compared with the sensed DC link voltage (V_{dc}) to create error signal. The error signal is given to the PI (proportional Integral) controller for generating the I_{dc} and is given as,

$$V_e(k)= V_{dc}^*(k)- V_{dc}(k) \tag{2.9}$$

$$I_{dc}(k)= I_{dc}(k\text{-}1) + k_p\{V_e(k)- V_e(k\text{-}1)\} +k_i*V_e(k) \tag{2.10}$$

Where k and (k-1) represent the kth and $(k-1)^{th}$ sampling instants. Here, the DC link voltage is maintained at 400V. The total active component of supply current is given as,

$$I_{active} =I_{dc}+K_1*I_b^* \tag{2.11}$$

10

Where, K1 is a constant needed to normalize the DC side power to the AC side and its value is given as,

$$K_1 = \sqrt{2} * \frac{V_b}{V_s} \tag{2.12}$$

Where V_s is the amplitude supply voltage, $V_s = \sqrt{V_\alpha{}^2 + V_\beta{}^2}$

A reactive component, $I_{reactive}$ is obtained from the PI controller loop of reactive power for tracking the Q_{cmd} as,

$$Q_e(k) = Q_{cmd}(k) - Q(k) \tag{2.13}$$

$$I_{reactive}(k) = I_{reactive}(k-1) + k_p\{Q_e(k) - Q_e(k-1)\} + k_i\,Q_e(k) \tag{2.14}$$

Where k and (k-1) represent the kth and $(k-1)^{th}$ sampling instants.

Now, using active and reactive components, the peak of supply reference current is calculated as,

$$I_{sp}^* = \sqrt{I_{active}{}^2 + I_{reactive}{}^2} \tag{2.15}$$

And finally the instantaneous reference supply current is estimated as,

$$i_s^* = I_{sp}^* * \sin(wt - \Theta) = I_{sp}^*\{sinwt * cos\Theta - coswt * sin\Theta\} \tag{2.16}$$

Where, wt is the phase angle of supply voltage obtained from the PLL. The gating pulses for IGBT of AC-DC converter are generated by processing the current error between the sensed supply current, i_s and reference grid current, i_s^* through hysteresis current controller.

2.4 RESULTS AND DISCUSSION

The proposed system parameters used in simulation is given in Appendix and the system is simulated for a single phase grid of 230V, 50 Hz. The Dc link voltage of AC-DC converter is maintained at 400 V for both the modes of operation. The battery ampere hour's capacity is large, therefore, the charging and discharging do not much affect the battery voltage. The simulation for G2V mode is explained here.

In G2V mode, for simulation, the active power command is considered as 2000Wand the reactive power command is considered as 1500VAR for unity PF, lagging PF and Leading PF respectively.

2.4.1 UNITY PF OPERATION

Fig.2.4 shows that the battery is being charged from the grid with a charging current of 6.75A and the power, P=2000W. Since the reactive power command 0VAR, therefore the current drawn from the grid is at UPF. The DC link voltage is maintained at 400V. The DC link voltage needs to be maintained at this voltage to transfer the power to the battery.
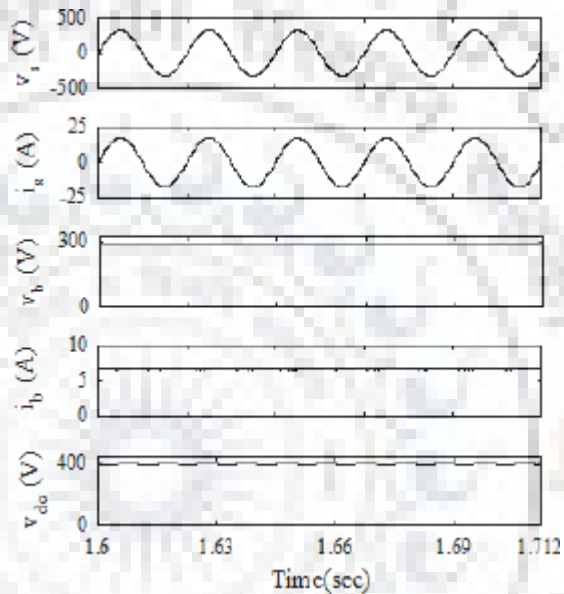

Fig.2. 4 G2V mode operation at P_{cmd}=2000W and Q_{cmd}=0 VAR

2.4.2 LAGGING PF OPERATION

Fig.2.5 shows that the battery is being charged from the grid with a charging current of 6.75A and the power, P=2010W. Since the reactive power command 1500VAR, therefore the current drawn from the grid is lagging the PCC voltage by an angle 27°. The DC link voltage is maintained at 400V. The DC link voltage needs to be maintained at this voltage to transfer the power to the battery. Here, it is to be noted that, the reactive power compensation is achieved by the charger while charging even without consuming active power from the battery.
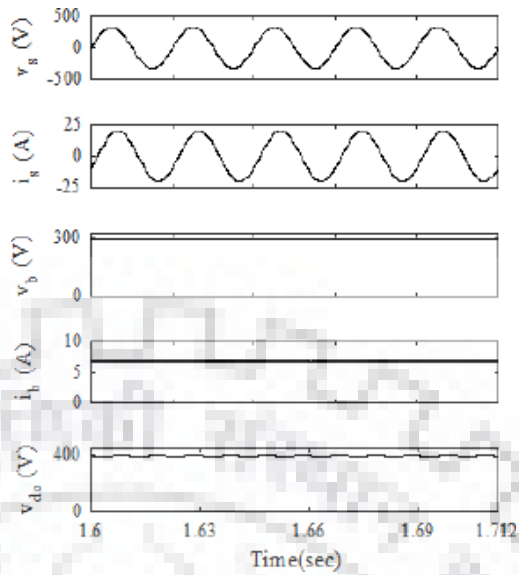
Fig.2. 5 G2V mode operation at Pcmd=2000W and Qcmd=1500 VAR

2.4.3   LEADING PF OPERATION

Fig.2.6 shows that the battery is being charged from the grid with a charging current of 6.75A and the power, P=2000W. Since the reactive power command -1500VAR, therefore the current drawn from the grid is leading the PCC voltage by an angle 27°. The DC link voltage is maintained at 400V. The DC link voltage needs to be maintained at this voltage to transfer the power to the battery. Here, it is to be noted that, the reactive power compensation is achieved by the charger while charging even without consuming active power from the battery.
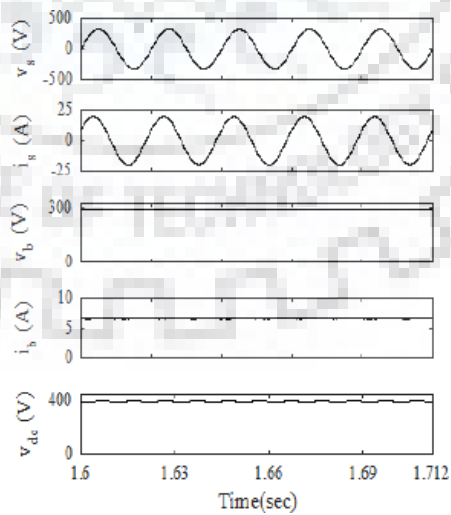

Fig.2. 6 G2V mode operation at Pcmd=2000W and Qcmd=−1500 VAR

13

Chapter 3

AN IMPLEMENTATION OF SOLAR PV ARRAY BASED MULTIFUNCTIONAL EV CHARGER

3.1 CHARGING STATION DESIGN

In this proposed bidirectional charger, the boost converter is eliminated, and the solar PV array is connected directly to the DC bus of VSC. Here, in this topology, the VSC fulfils the task of harnessing maximum power from the solar PV array. Therefore, this charger is a retrofit solution to the existing single phase bi-directional charger with a modification in the control algorithm. The proposed charger has following distinctive features.
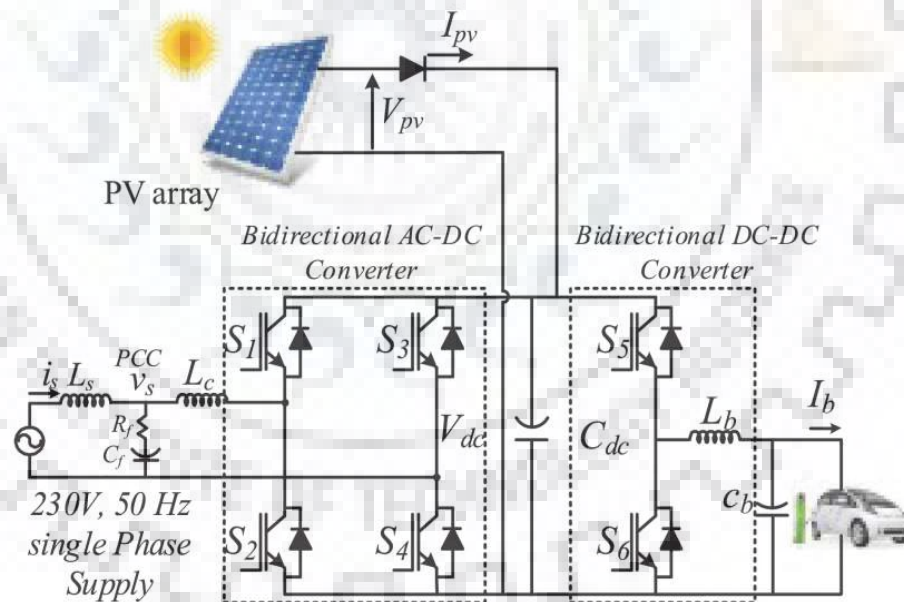

Fig.3. 1 System configuration of the proposed charger

- It uses the solar PV energy to charge the EV battery and uses the grid in case of insufficient the solar PV energy. The controller decides when to use the solar PV energy and when to use the grid energy.

- Along with the active power trade with the utility, the charger exchanges the reactive power with the grid using the VSC of the charger. Both active and reactive powers exchanges are possible even when the EV is not connected to the charger.

- The proposed charger eliminates the DC-DC boost converter used for MPPT in the conventional charger.

- While exchanging the active and reactive powers, the grid current THD remains within the limits of the IEEE 519 standard.

- To use the solar PV array efficiently, the control algorithm extracts the maximum power at all irradiance levels.

3.2 SYSTEM CONFIGURATION

The circuit topology of the proposed system is shown in Fig.3.1. This system is a single phase bi-directional charger for an EV that integrates the solar PV array directly on the DC bus of the VSC. The proposed charger charges the EV battery using the solar PV power/the grid power and feeds the solar PV / EV battery power into the grid. The proposed charger is a two stage charger, i.e. a bi-directional AC-DC conversion followed by the bi-directional DC-DC conversion stage. The AC-DC conversion stage converts the input AC voltage into the DC voltage while charging the EV battery and works as an inverter to change the DC voltage into the AC voltage while feeding the solar PV power and EV power into the grid. The EV battery is connected to the output of the bi-directional DC-DC converter (BDDC). The DC-DC converter in this charger accomplishes the various tasks. While charging the EV battery, the DC converter works in buck mode and operates in boost mode while discharging the EV battery. Moreover, it also regulates the DC bus voltage and harnesses the maximum generated power from the solar PV array. The proposed charger is connected to the grid through the coupling inductor (L_c). A coupling inductor is needed to eliminate the harmonics and to smoothen the grid current. A ripple filter is also connected at the PCC (Point of Common Coupling) to prevent the injection of switching harmonics generated by the switching of VSC into the grid.

3.3 CONTROL ALGORITHM

The charger is controlled to perform these required functions as follows, 1) energy balance in the system, 2) harnessing of maximum solar PV array power, 3) generation of reference grid current for both active and reactive power flow, 4) charging/discharging current control of EV by controlling the bi-directional DC-DC converter. The energy balance in the system and harnessing of maximum solar PV array power are attained by regulating the DC bus voltage. However, the active/reactive power control is achieved by the grid current control. The overall control of the charger is designed as, 1) energy management strategy of charger, 2) VSC control, and 3) bi-directional DC-DC converter control.

3.3.1 ENERGY MANAGEMENT STRATEGY OF THE PROPOSED CHARGER

The energy management strategy of the proposed charger is based on the constant DC bus capacitor voltage. The flow chart of the energy management under different operating conditions is shown in Fig.3.2. The energy management in steady state is given as,

$$P_{PV} \pm P_B \pm P_S = 0 \tag{3.1}$$

Here PPV, PB and Ps are solar PV array power, EV power and grid power, respectively. In this expression, the positive power represents the supplying of power, and negative power represents the consumption of power. This means that the EV and the grid can both supply and consume the power. The charger undergoes the transient caused by the change in solar irradiance and change in charging demand. The dynamic power management equation in case of solar irradiance change is given as,

$$\Delta P_{PV} \pm \Delta P_B \pm \Delta P_S = 0 \tag{3.2}$$

Since the solar irradiance is changing throughout the day, the charging of the EV battery should not be affected. Therefore, based on the energy management strategy, a series of event occurs to achieve the energy equilibrium in the system.

Solar irradiance $\uparrow \quad \rightarrow P_{PV} \uparrow \rightarrow$ power at DC link $\uparrow$

$$\rightarrow V_{DC} \uparrow \quad \rightarrow V_{DC} \text{regulation} \rightarrow I_P \quad \uparrow \rightarrow i_s^* \uparrow \tag{3.3}$$

Similarly, the energy management in case of decreased solar irradiance is achieved as,

16

Solar irradiance↓ → P_{PV} ↓ → power at DC link ↓ → V_{DC} ↓ → V_{DC} regulation

→ I_P ↓ → i_s^* ↓   (3.4)

With the load change, the solar PV array power should not be affected, and series of events for energy management during these transients are as follows,

Charging Power↓ → I_B↑→power at DC link ↓

→V_{DC}↓→V_{DC}regulation → I_P↓→i_s^*↓   (3.5)

Charging Power↓ → I_B↓→power at DC link ↑

→V_{DC}↑→V_{DC}regulation → I_P↑→i_s^*↑   (3.6)

3.3.2 VSC CONTROL

The VSC control diagram is shown in Fig.3.3. The purpose of the VSC control is to regulate the DC bus voltage and control the grid current for controlling the active and reactive power flow, thereby generating the switching pulses for the VSC. The DC bus voltage regulation is achieved by a proportional integral (PI) controller used for minimizing the error between actual DC bus voltage (V_{dc}) and reference DC bus voltage ($V_{dc}*$). The MPPT (Maximum Power Point Tracking) algorithm estimates the reference DC bus voltage ($V_{dc}*$) at which the peak power of the solar PV array is extracted. In the absence of the solar PV generation, the DC link voltage is regulated at 360V. The DC link reference voltage ($V_{dc}*$) is compared with the sensed DC link voltage (V_{dc}). The error voltage (V_e) of the DC link voltage, is the input of the PI (Proportional Integral) controller. The output of the PI controller gives the magnitude of the real power constituent (I_P) of the reference grid current (i_s*). The expression of PI controller in the discrete domain is given as,

$I_P(k)= I_P(k-1) + k_p\{V_e(k)- V_e(k-1)\} + k_i*V_e(k)$ (3.6)

Where $V_e=V_{dc}*-V_{dc}$, k and (k-1) are sampling instants and k_{pd} and k_{id} are the proportional and integral gains of the controller. The amplitude of the reactive power constituent (I_P) of the reference grid current (i_s*), is obtained based on the reference reactive power command (Q_{cmd}) and it is given as,

$I_q=\frac{2*Q_{cmd}}{V_{tm}}$ (3.7)

Where Q_{cmd} is the reference reactive power command. Whereas V_{tm} is the peak amplitude of the PCC voltage (v_s).

The real (I_P)) and reactive (I_q)) components are multiplied with the in-phase (u_P) and the quadrature phase unit template (u_q)) to obtain instantaneous reference active grid current (i_P)) and instantaneous reference reactive grid current (i_q)), and it is given as,

$$i_p = I_P * u_p \, , \; i_q = I_q * u_q \tag{3.8}$$

The in-phase (u_P) and the quadrature phase unit template (u_q) are obtained using the following expressions

$$u_p = \frac{v_\alpha}{V_{tm}} \, , u_q = \frac{v_\beta}{V_{tm}} \tag{3.9}$$

Where v_α and v_β are the in-phase and quadrature phase voltage of PCC voltage (u_s). It is generated using the quadrature signal generator.
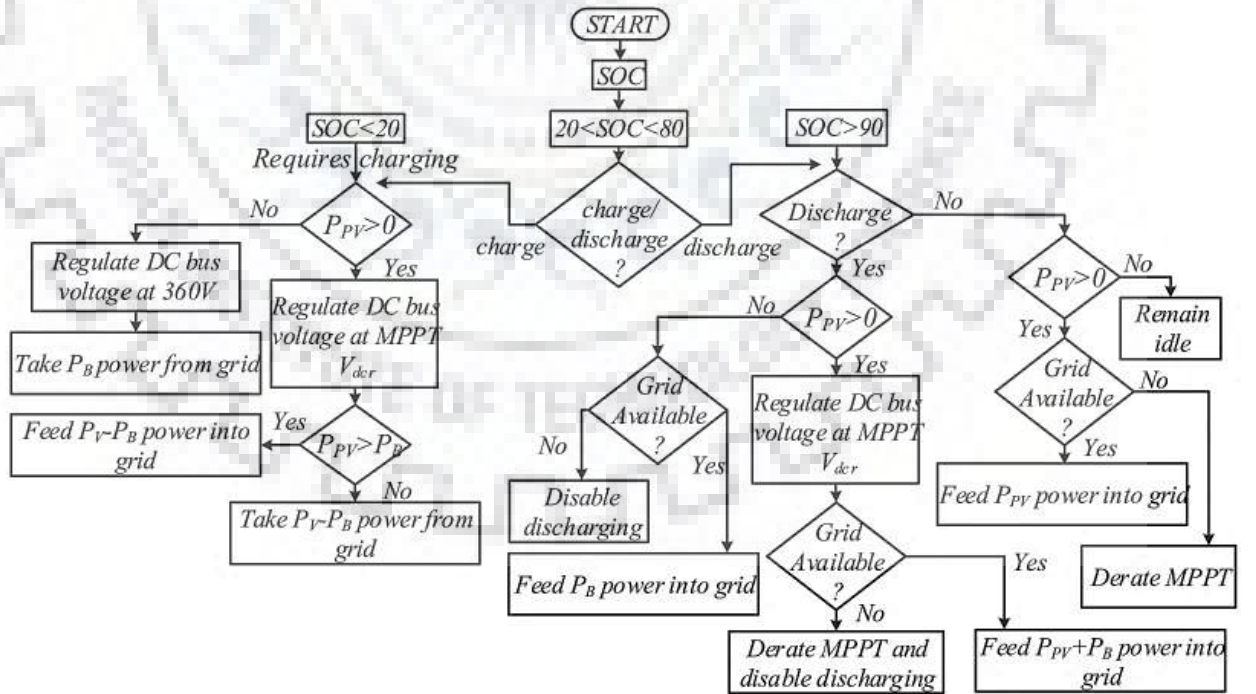

Fig.3. 2 Power management strategy.

Using reference active grid current (i_p) and reference reactive grid current (i_q), the total reference grid current is obtained as,

$$i_s^* = i_p + i_q \tag{3.10}$$

This reference grid current (i_s*) is compared with the sensed grid current (i_s) and the hysteresis controller generates the triggering signals for the VSC.
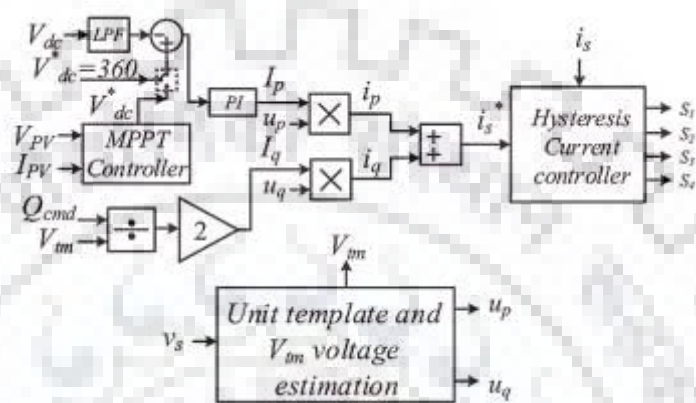

Fig.3. 3 Control Diagram for VSC.

3.3.3 BI-DIRECTIONAL DC-DC CONVERTER CONTROL

The control diagram for the bi-directional DC-DC converter is shown in Fig.3.4. Based on the power demand for the charging of EV battery, the reference charging current (I_b*) is estimated. After that, a PI controller is used to regulate the EV current at the reference value. The output of the PI controller gives the duty cycle of the DC-DC converter and PWM modulator generates the switching pulses for the converter.
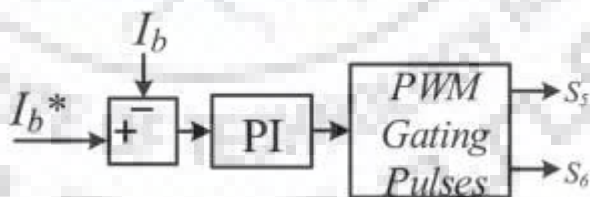

Fig.3. 4 Control diagram of DC-DC converter.

3.4 RESULTS AND DISCUSSION

The charger is designed for single phase 230V, 50Hz supply system. The open circuit voltage and short circuit current of solar PV array is 425V and 7A, respectively. However, the maximum

power point voltage and current are 366 V and 6.6A, respectively. The lead-acid battery of 240V, 35Ah is used as an EV battery in the experimental prototype. The implementation of the proposed charger is done using the digital controller (dSPACE −1006). For the implementation of the control algorithm, the digital controller requires various (voltage and current) signals of the charger. Therefore, various voltage and current signal (analog) are acquired using the Hall Effect based voltage and current sensor. These signals are then converted into a digital signal using analog to digital converter (ADC).The digital controller uses the digital signal to implement the control algorithm and generate the switching pulses for VSC and DC-DC converter. The experimental waveforms of the proposed charger are shown in Figs.3.5– 3.11. The performance of the proposed charger is evaluated in both steady state and dynamic conditions. In steady state conditions, various modes of operation are considered such as, 1) EV is not connected to the charger and whole solar PV array generated power is fed into the grid, 2) the grid is not available and solar PV array generated power is consumed by the EV, 3) reactive power compensation of the charger along with the active power operation, and 5) solar PV array supplying power to EV and feeding power into the grid. The dynamic performance is evaluated under solar irradiance change and change in the battery charging current. During implementation, the solar PV array power (P_{PV}), the power is drawn from the grid (P_s), the power drawn from the battery (P_B), are considered positive. However, the power fed into the grid and the battery is considered negative.

3.4.1 STEADY STATE PERFORMANCE OF PROPOSED CHARGER

The performance in the case when the state of charge (SOC) of the EV battery is more than 80%, and solar PV array is generating maximum power, are shown in Fig.3.5. In this case, to avoid the overcharging of the EV battery and to utilize the solar PV array energy fully, the charger feeds the solar PV energy into the grid using VSC. Figs.3.5 (e)-(f) show that the solar PV array is generating 2.32kW. Out of 2.32kW, 2.29kW is fed into the grid at UPF. The voltage (V_{PV}), current (I_{PV}) and power (P_{PV}) of the solar PV array, are shown in Figs.3.5 (e)-(f). However, the voltage (v_s), current (i_s), and power (P_s) of the grid are shown in Figs.3.5 (a)-(b). The charger is not injecting any voltage and current harmonics into the grid (despite the charger is having power electronic component), as shown by the grid voltage (v_s) and current (i_s) total harmonic distortion (THD) in Figs.3.5(c)-(d). Moreover, it is also not drawing any reactive power from the grid as justified by the unity displacement power factor (DPF) operation of the charger in Fig.3.5 (b).

When the EV battery is discharged, and its SOC reaches below 20%, the EV battery takes power from the solar PV array for charging in the absence of the grid. The performance under this case is shown in Fig.3.6. The voltage (V_B), current (I_B) and power of the EV battery (P_B) are shown in Fig.3.6 (a), (b). However, the voltage (V_{PV}), current (I_{PV}) and power of solar PV array (P_{PV}) are shown in Fig.3.6 (c), (d).

During the day hour, sometimes the solar PV array generated power (PPV) becomes more than the charging demand (PB) due to increased solar irradiance level or decreased charging demand. In this condition, the power management strategy of the charger automatically feeds the surplus solar PV array power into the grid without derating the MPPT performance or altering the charging demand. The performance under this condition isshown in Fig.3.7. The EV battery is taking 1.38kW of 2.44kW of solar PV generated power. The voltage (VB), current (IB) and power of the EV battery (PB) are shown in Figs.3.7 (e), (f). The solar PV array power is displayed in Fig.3.7 (g). Since the solar PV array power (PPV) is fed into the grid, the controller of the charger synchronizes the PCC voltage with the grid voltage as per the control algorithm is shown in Figs.3.7(a) - (b) show that the 898W is fed into the grid at UPF. The performance of the charger while feeding power into the grid in terms of THD of the voltage (vs) and current (is) are exhibited in Figs. 3.7(c) - (d). It shows that the THD of the grid voltage and current are less than 5% thus achieving the IEEE519 standard.
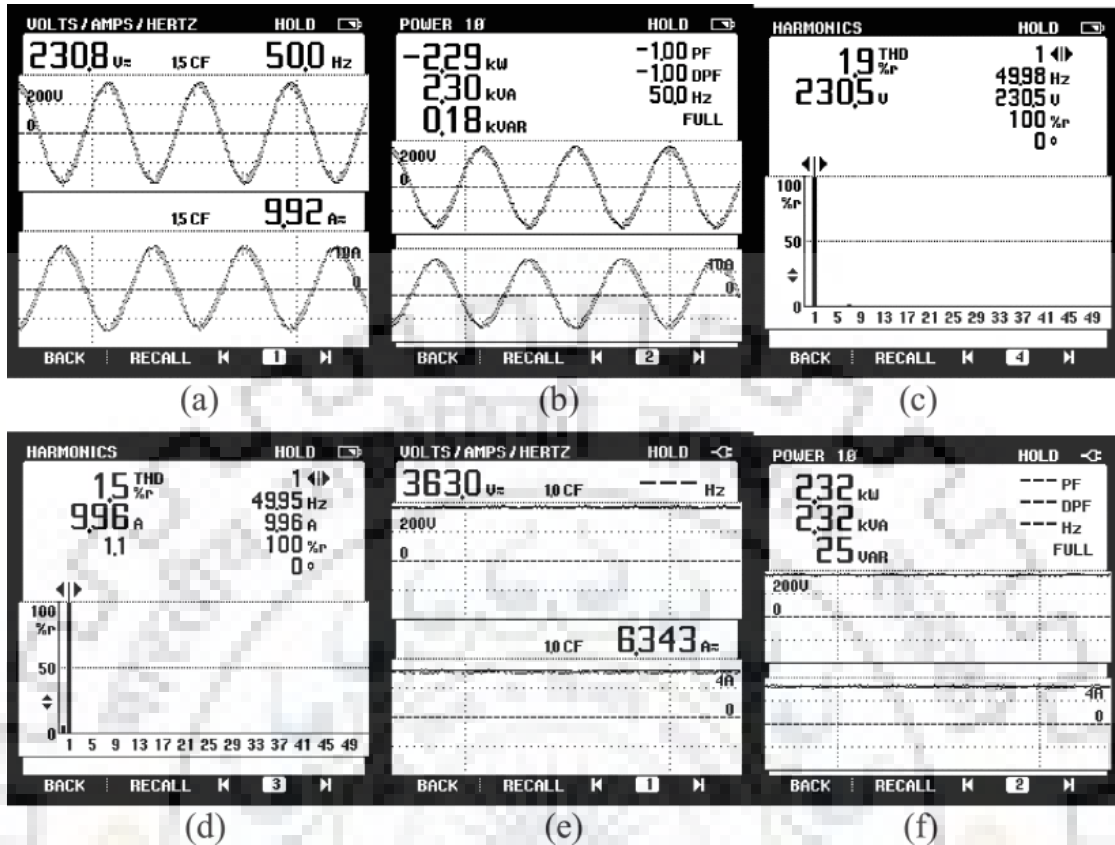
VOLTS/AMPS/HERTZ HOLD	POWER 1θ HOLD	HARMONICS HOLD
2308 v= 15 CF 50.0 Hz	-2.29 kW -1.00 PF	1.9 THD 1
200V	2.30 kVA -1.00 DPF	%r 4998 Hz
0	0.18 kVAR 50.0 Hz FULL	2305 v 2305 v 100 %r 0°
15 CF 9.92 A=	200V 0	100 %r 50
		0 1 5 9 13 17 21 25 29 33 37 41 45 49
BACK RECALL (1)	BACK RECALL (2)	BACK RECALL (4)
(a)	(b)	(c)

HARMONICS HOLD	VOLTS/AMPS/HERTZ HOLD	POWER 1θ HOLD
1.5 THD 1	3630 v= 1.0 CF --- Hz	2.32 kW --- PF
%r 49.95 Hz	200V	2.32 kVA --- DPF
9.96 A 9.96 A	0	25 VAR --- Hz FULL
1.1 100 %r 0°	1.0 CF 6.343 A=	200V 0
100 %r 50	4A 0	4A 0
0 1 5 9 13 17 21 25 29 33 37 41 45 49		
BACK RECALL (3)	BACK RECALL (1)	BACK RECALL (2)
(d)	(e)	(f)

Fig.3. 5 Performance of solar PV feeding power into the grid when EV battery is fully charged, (a) v_s and i_s, (b) P_s, (c)-(d) THDs of v_s and i_s, (e) V_{pv} and I_{pv}, (f) P_{PV}

The performance of the charger while feeding both solar PV array and EV battery powers into the grid is shown in Fig.3.8. During the peak demand of the grid, the charger uses both solar PV array energy and EV energy to support the grid. Fig.3.8 (a) - (b) show that the 2.97kW is fed into the grid using the solar PV array and EV energy. The EV is feeding 815W .Fig.3.8 (e) - (f)) and remaining power is coming from the solar PV array. In this case, also, the THDs of the grid voltage (vs) and current (is) (Fig.3.8 (c) - (d)) are less than 5% as required by the IEEE 519 standard.

22
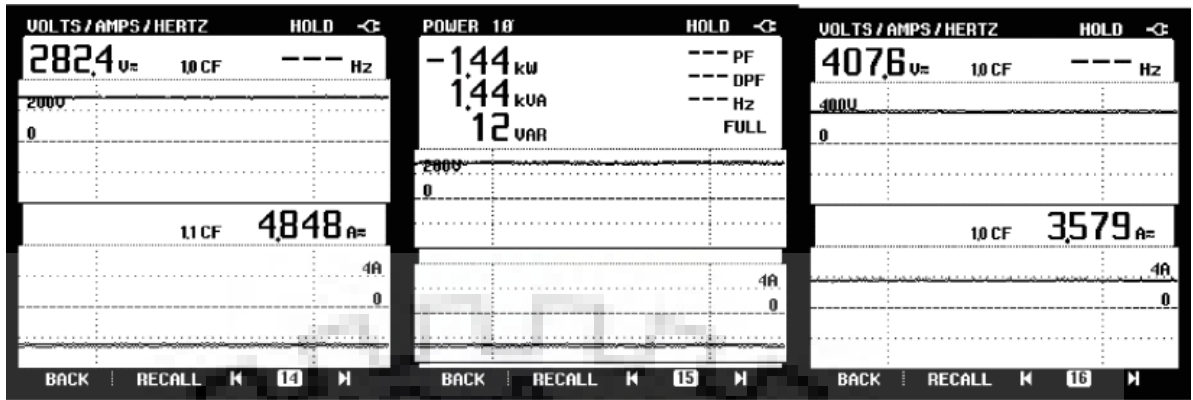
Fig.3. 6 Performance of charger when charging EV battery in absence of grid, (a) V_b and I_b, (b) P_B, (c) V_{pv} and I_{pv}, (d) P_{PV}
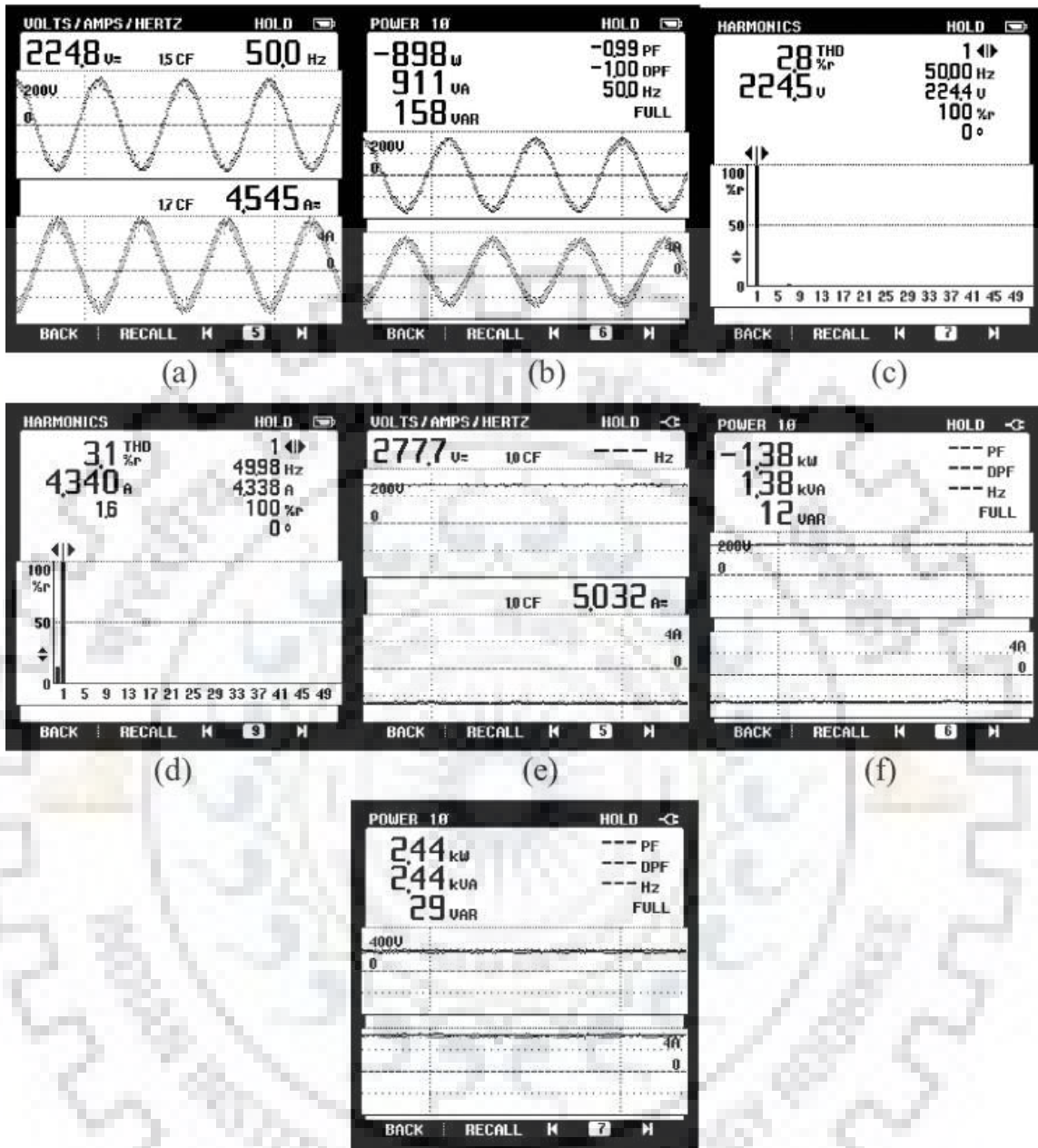
Fig.3. 7 Performance of charger when feeding solar PV power into grid and charging EV battery, (a) v_s and i_s, (b) P_s, (c)-(d) THDs of v_s and i_s, (e) V_b and I_b, (f) P_B, (g) P_{PV}
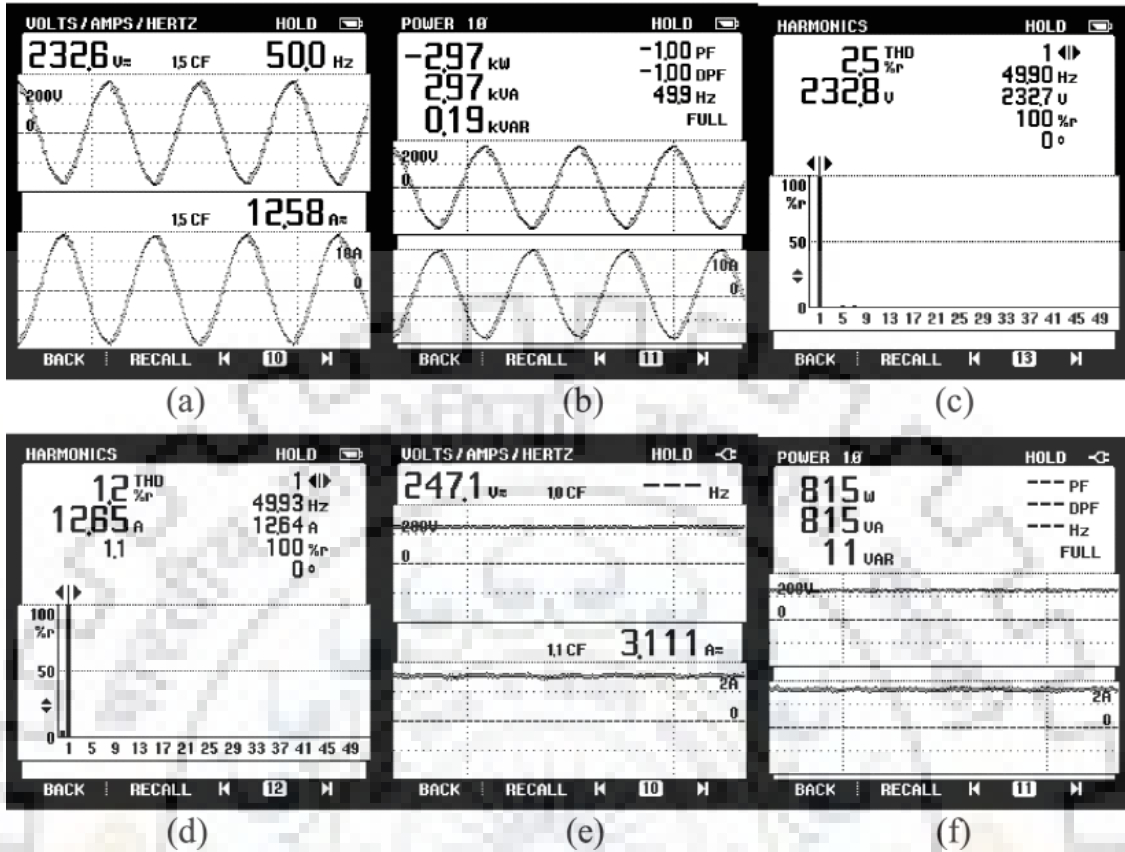
Fig.3. 8 Performance of charger when feeding solar PV power and EV power into the grid, (a) vs and is, (b)Ps,(c)−(d) THDs of vs and is, (e) Vb and Ib, (f) PB

The charger capability to provide reactive power support along with the active power flow is shown in Fig.3.9 .On demand of the grid, the charger also supplies the reactive power (inductive/capacitive) to the grid along with the active power. The charger is drawing 910VAR of inductive reactive power from the grid while feeding 1.42kW active power into the grid. Due to the reactive power compensation, the charger is operating at 0.85PF as shown in Fig.3.9. The voltage (vs), current (is) and power (Ps) of the grid while flowing both active and reactive powers, are shown in Fig.3.9 (a) - (b). The THDs of grid voltage (vs) and current (is) are 2.6% and 1.8%, respectively as shown in Fig.3.9 (c) - (d). Fig.3.9 (e) - (f) show the EV voltage, current and power.
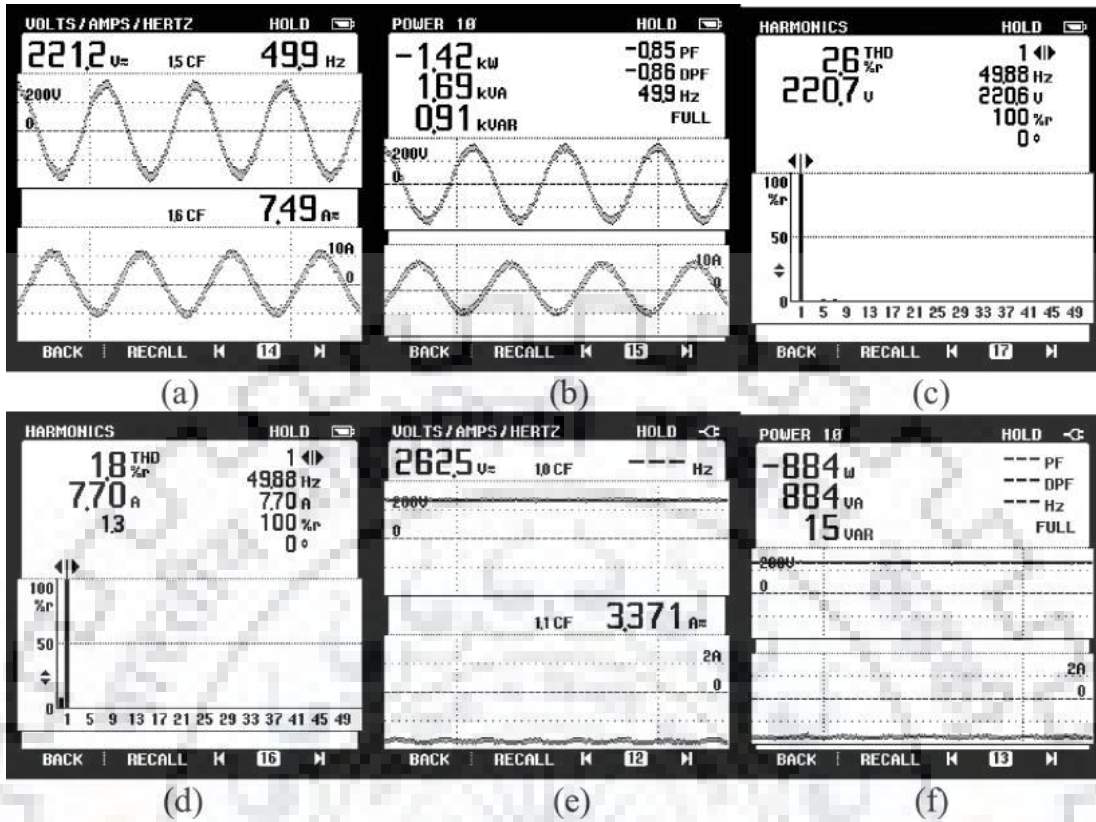
Fig.3. 9 Simultaneous active and reactive power operation during battery charging from solar PV, (a) vs and is, (b) grid active and reactive power, (c)-(d) THDs of vs and is, (e) Vb and Ib, (f) PB

3.4.2 DYNAMIC PERFORMANCE OF PROPOSED CHARGER

During the operation, the charger is subjected to the transient caused by the continuously changing solar irradiance level due to the shading of the clouds and the change in the charging demand. Under these two transient conditions, the charger and the control of the charger should operate such that the maximum power is harnessed from the solar PV array at all irradiance level without disturbing the charging of the EV. Moreover, the flow of active power should be balanced in the system during transients. The performance under step change in solar irradiance level from 1000W/m2 to 500W/m2 and vice versa are exhibited in Fig.3.10 Fig.3.10 (a)-(b) show the performance under step change in solar irradiance intensity from 1000W/m2 to 500W/m2. Due to a decrease in the solar irradiance intensity, the solar PV current (IPV) decreases. Moreover, the DC bus voltage (Vdc) also decreases from 372V to 351V to extract the maximum power at 500W/m2. As a result, the solar PV generated power (PPV) decreases from 2.4kW to 1.2kW. As the charging of EV is undisturbed (as shown from IB in Fig.3.10 (a)), the power which is being fed into the grid decreases. Therefore, the grid current

26

(is) reduces as shown in Fig.3.10 (a). Similarly, in case of an increase in solar irradiance from 500W/m2 to 1000W/m2, the solar PV array power (PPV) increases from 1.2kW to 2.4kW as exhibited in Fig.3.10 (c). In this condition, the DC bus voltage (Vdc) increases from 351V to 372V to continue the process of maximum power extraction. However, the charging of the EV does not get affected by the solar irradiance increase as shown by IB in Fig.3.10 (d).

The performance under change in charging current is shown in Fig.3.11 (a)-(c). Under this dynamic change, the charging current (IB) is decreased from 3A-1.5A and again it is increased from 1.5A-3A. Since the charging current (IB) of EV is decreased from 3A-1.5A, the energy management strategy maintains the power balance by feeding the extra power into the grid without disturbing the MPP operation of the solar PV array. Because of this, the grid current (is) increases as shown in Fig.3.11 (a). Similarly, when the charging current (IB) in increased from 1.5A to 3A, the grid current (is) reduces to maintain the power balance as solar PV array cannot supply more power as presented in Fig.3.11 (b). Moreover, the DC bus voltage (Vdc) does not get affected by this disturbance as exhibited in Fig.3.11 (c).
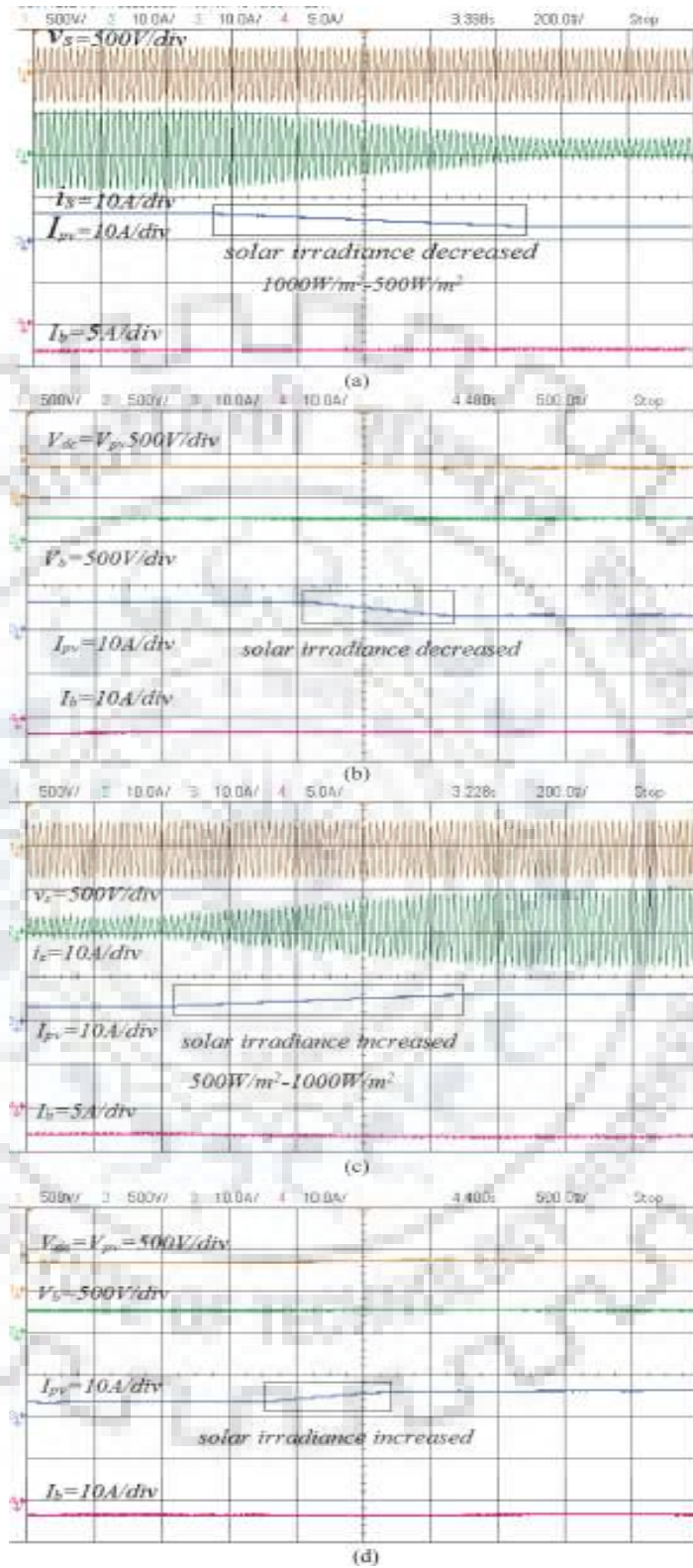
Fig.3. 10 Performance of charger under solar irradiance change, (a)-(b) solar irradiance decrease from 1000W/m2 500W/m2, (c)-(d) solar irradiance increase from 500W/m2-1000W/m2
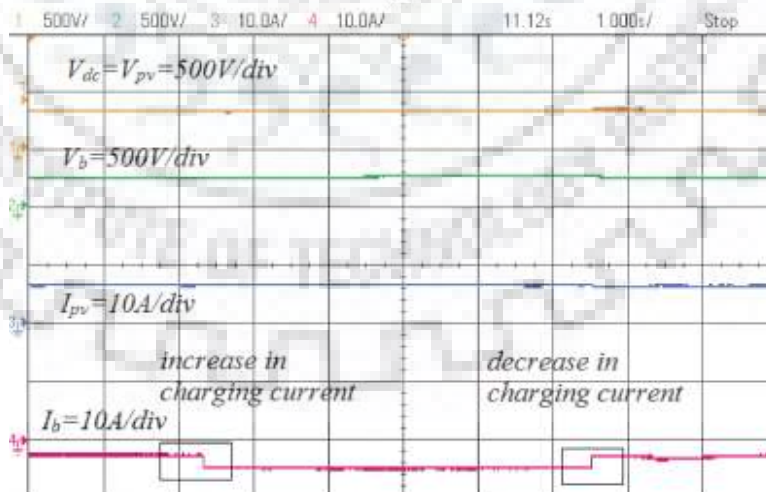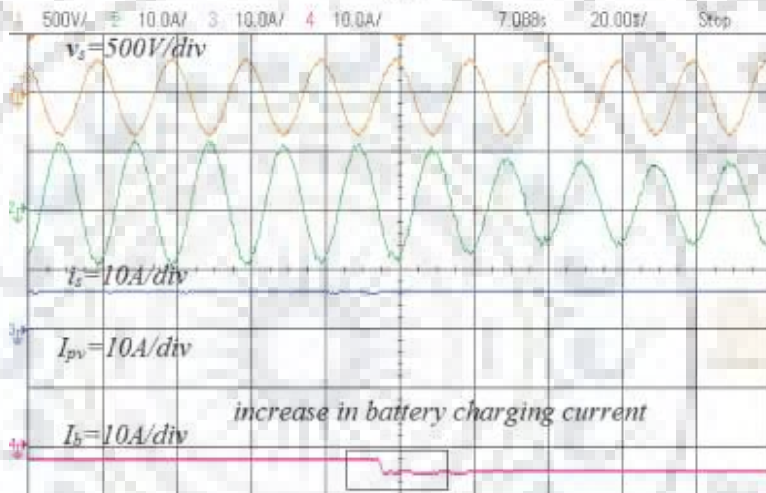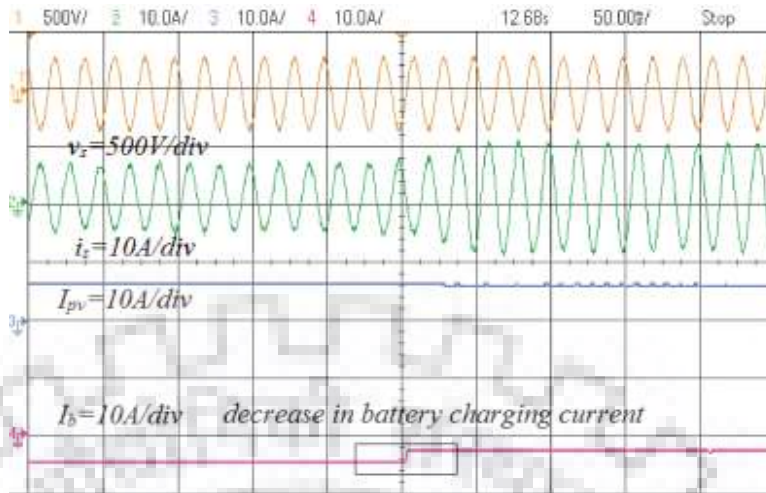
28

Fig.3. 11 Performance of the charger under change in battery current, (a) decrease in charging current from 3A-I.5A, (b) increase in charging current 1.5A-3A, (c) combined waveforms

Chapter 4

CASE STUDIES INVOLVING SIMULATION AND RESULTS

4.1   INTRODUCTION

Here in the part 1 description about one phase EV charger configuration along with control strategy are presented. Simulations results for EV charger in grid to vehicle mode are shown, which assures quality power consumptions from grid. Similarly in the part 2 solar PV array based multifunctional EV charger MATLAB simulation model along with corresponding control diagram are discussed. In the later part related results are presented.

4.1   MATLAB RESULTS (PART 1) WITH SIMULINK MODEL.

 Fig. 4.1 shows Simulink model of the bi-directional converter based EV charger. The main four parts are AC-DC converter, DC-DC buck-boost converter, and main control circuit and li-ion battery. The control circuit of the EV charger give the gating pulses to the both the converters through PWM circuits. The inputs to the control circuits are grid voltage (Vs), grid current (is), DC-link voltage (Vdc), battery voltage (Vb) and battery current (Ib).The active power input is fixed at 800W and reactive power input at 300VAR. Reference DC-link voltage is fixed at 253V.One set of gate pulses given to AC-DC converter switches and another set to the DC-DC buck-boost converter in constant voltage control mode in G2V mode which is shown in Fig.4.2. Fig.4.3 shows battery current during charging of battery from grid. It is fixed almost near to 3A due to proper control strategy in DC-DC converter. Battery voltage also is maintained at 265V during V2G mode which is shown in Fig.4.4. As both active and reactive powers are drawn from grid, so the grid current is lagging in nature. Similarly other two cases (i.e. unity power factor and leading power factor condition) can be verified through this Simulink model. Here one advantage is reactive power compensation can be achieved during charging but not consuming active power.
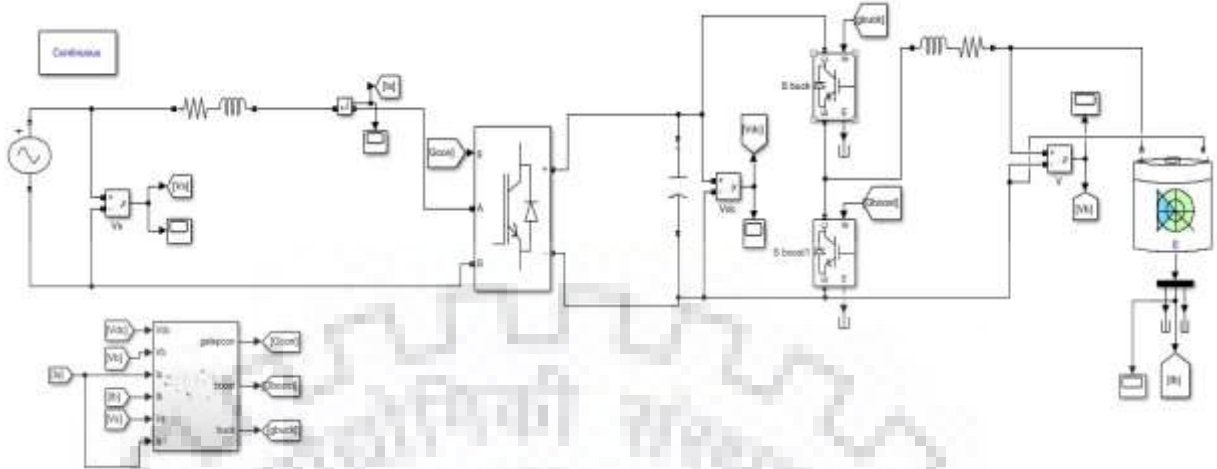
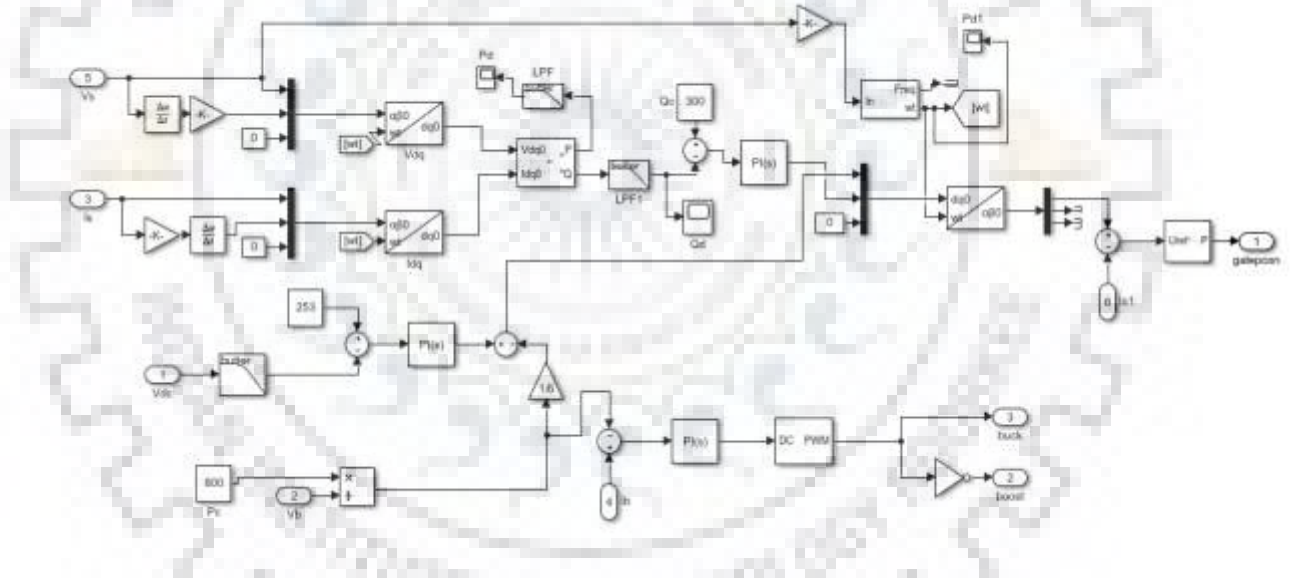Fig.4. 1 Simulink model of EV charger in G2V mode

Fig.4. 2 Control circuit in G2V mode

The results associated with the simulation are shown in figures starting from fig.4.3 to 4.6. The FFT analysis of input current gives THD percentage about 8.94%. This implies that electric vehicle battery takes power with injection of very small amount of harmonics to system and the THD limit is almost in margin with the THD (Total Harmonic Distortion) limit set by IEEE 519 standard.

The most important thing is the DC-link voltage should remain constant irrespective of power flow and that is done by deciding the DC link capacitor and proper control. Here in Fig.4.5, it is shown that DC link voltage is made fix at 254V.At last the grid current which is shown in Fig.4.15 is most likely as sine wave , which validate the simulation by satisfying the required condition.
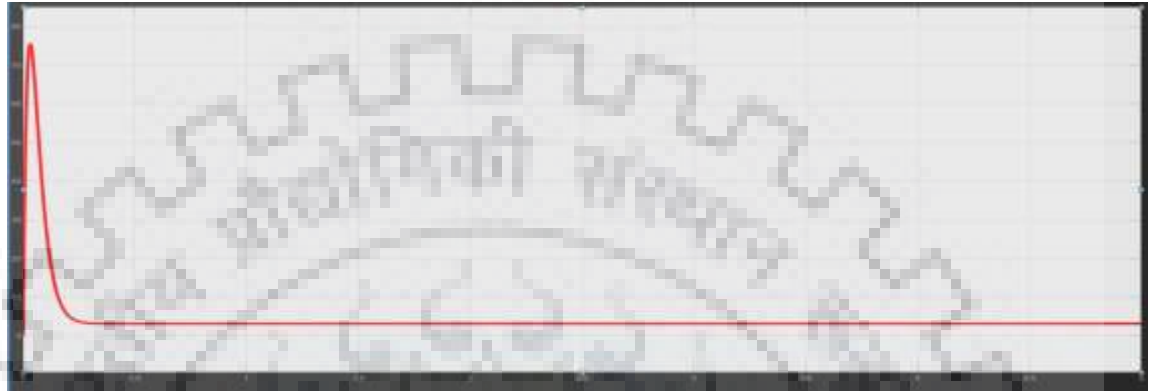

Fig.4. 3 Battery Current in Amps.
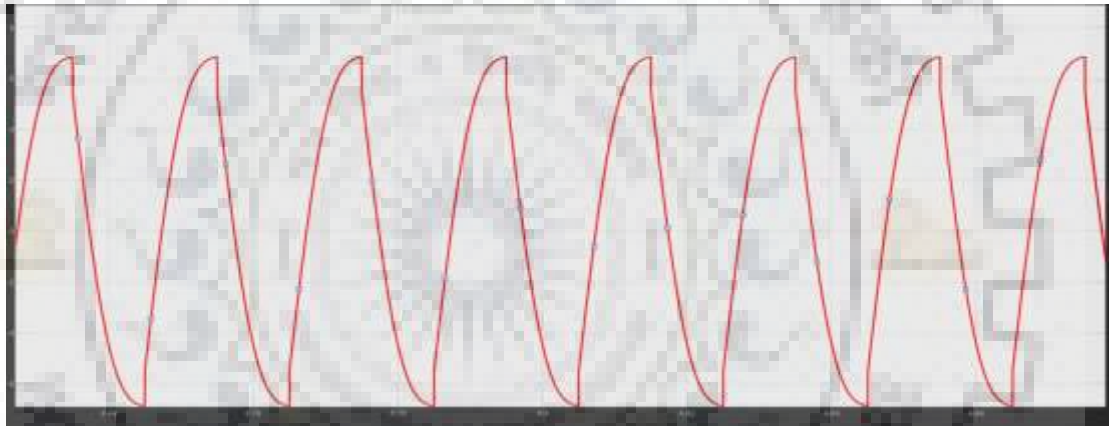

Fig.4. 4 Battery Voltage in Volts.

Fig.4. 5 DC link voltage in Volts.

Fig.4. 6 Input Current in Grid side having **THD 8.94%**

4.2   MATLAB RESULTS (PART 2) WITH SIMULINK MODEL.

In this part the charger is designed for single phase 230V, 50Hz supply system. The open circuit voltage and short circuit current of solar PV array is 425V and 7A, respectively. However, the maximum power point voltage and current are 360 V and 5.5A, respectively. The lead-acid battery of 250V, 10Ah is used as an EV battery in the experimental prototype which is shown in Fig.4.7. The experimental waveforms of the proposed charger are shown in Fig4.11-4.15. The performance of the proposed charger is done in steady state condition only. In steady state conditions, various modes of operation are considered such as 1) the grid is not available and solar PV array generated power is consumed by the EV and 2) solar PV array supplying power to EV and feeding power into the grid.

33

During day period when the EV battery is discharged, and its SOC reaches below 20%, the EV battery takes power in the absence of grid. In Simulink this is done by enabling the solar power in the control circuit part. Mostly the power management strategy decides when to use only solar, only grid and when to use both the source depending upon the algorithm condition.

We can see the solar cell output is directly connected to DC-link without use of DC-DC boost converter and having zero variation of the behaviour. It all happened because of MPPT control algorithm is implemented in VSC control of AC-DC converter.
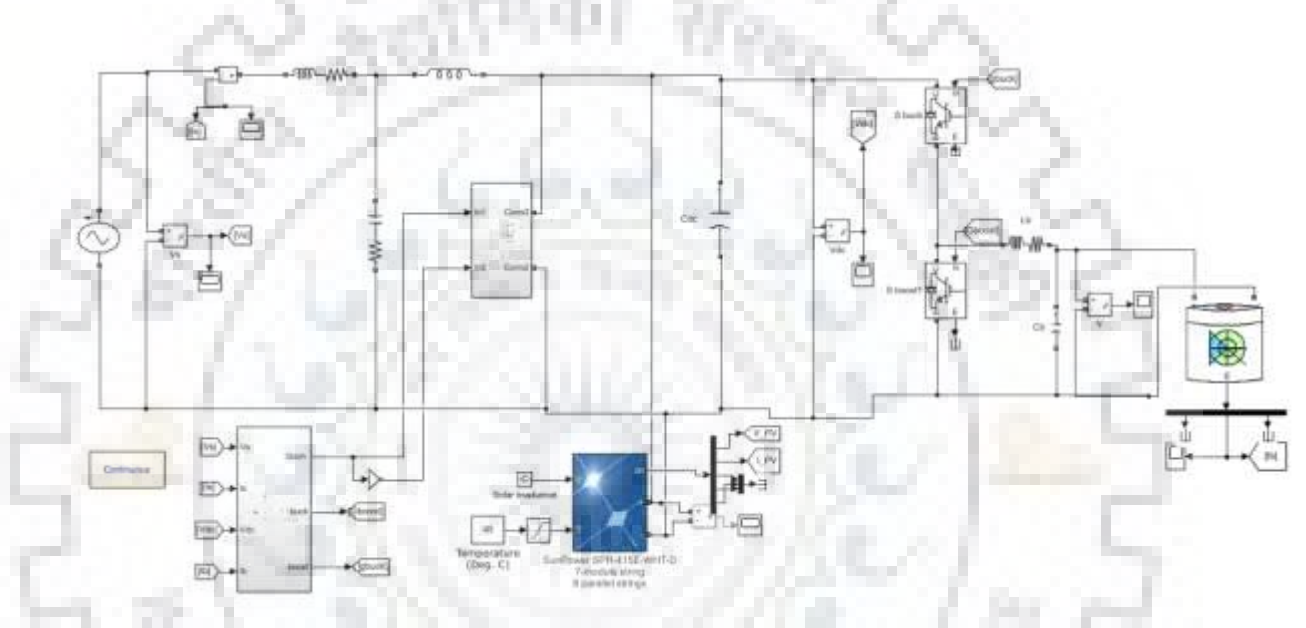
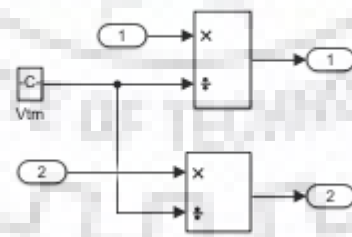Fig.4. 7 Simulink model of EV charger with solar PV panel and AC grid

Fig.4. 8 Unit template and V_{tm} estimation

The unit template and V_{tm} calculation was done in equation (3.7) and equation (3.9). Its outputs are used for calculation of reference grid current signal, which then compared with actual grid current and finally fed to a PI (Proportional -Integral) controller for generation of gate pulses for converter.
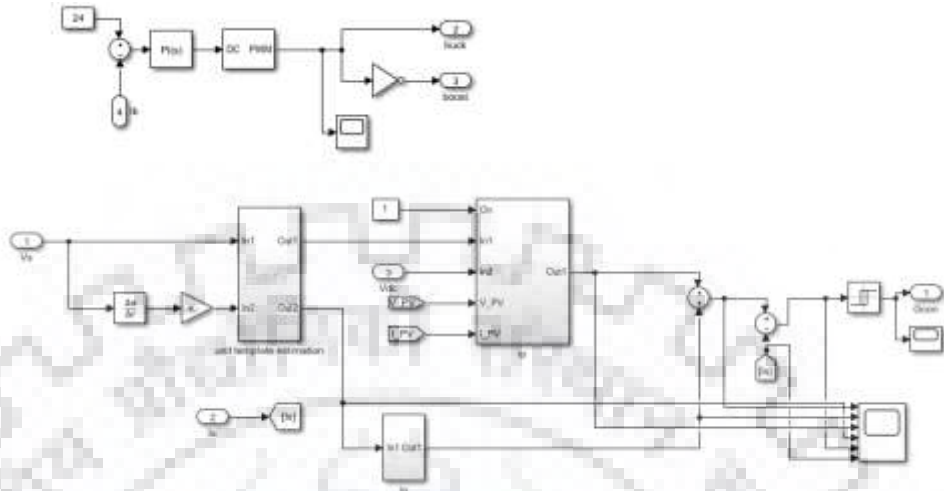
34

Fig.4. 9 Main Control circuit for both AC-DC converter and DC-DC converter
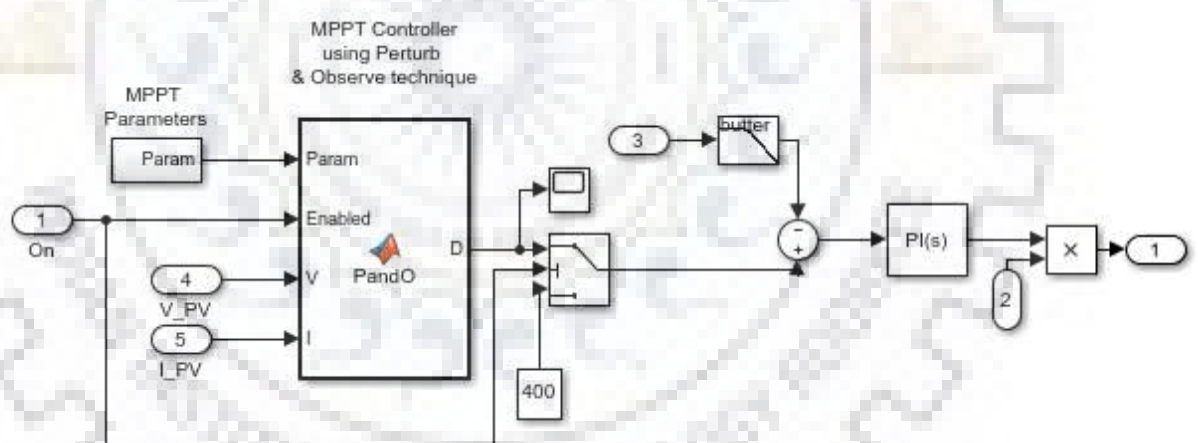

Fig.4. 10 Control circuit for I_p formation

The results associated with the simulation are shown in figures starting from fig.4.11 to 4.15. The FFT analysis of input current gives THD percentage about 9.7%. This implies that electric vehicle battery takes power with injection of very small amount of harmonics to system and the THD limit is almost in margin with the THD (Total Harmonic Distortion) limit set by IEEE 519 standard.
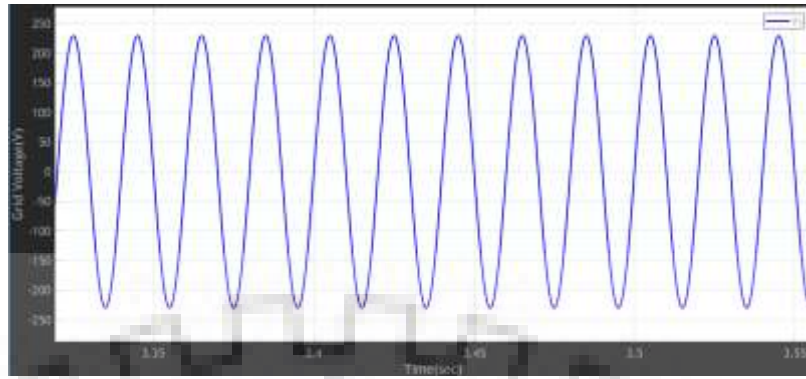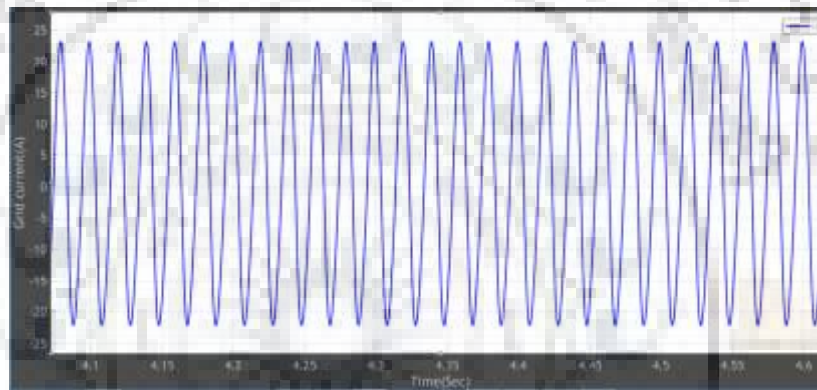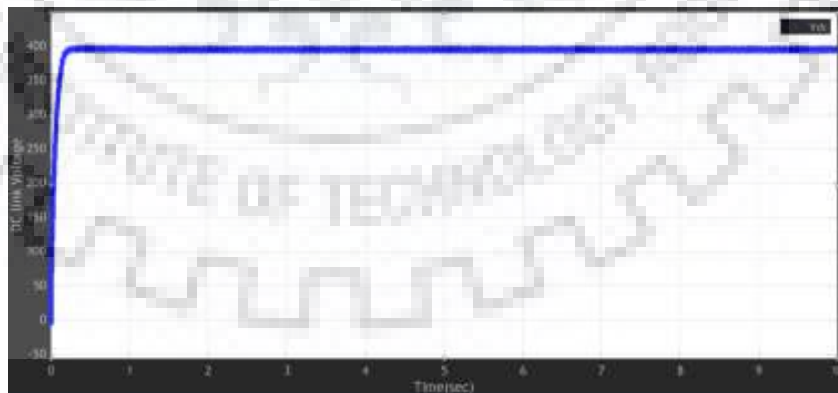
Fig.4. 11 Grid Voltage
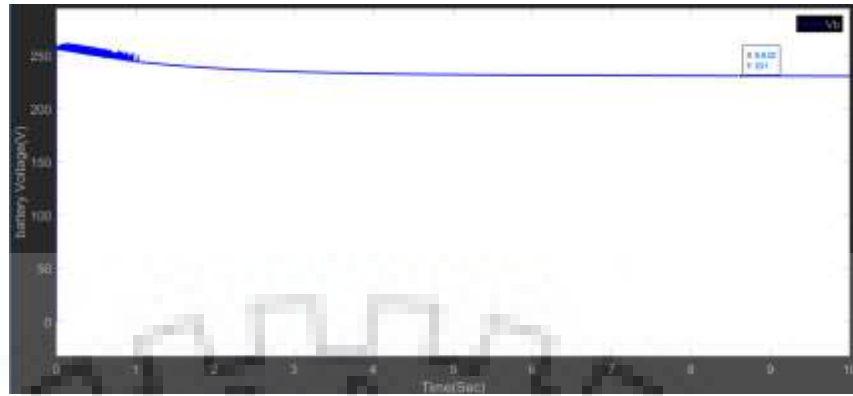

Fig.4. 12 Grid current
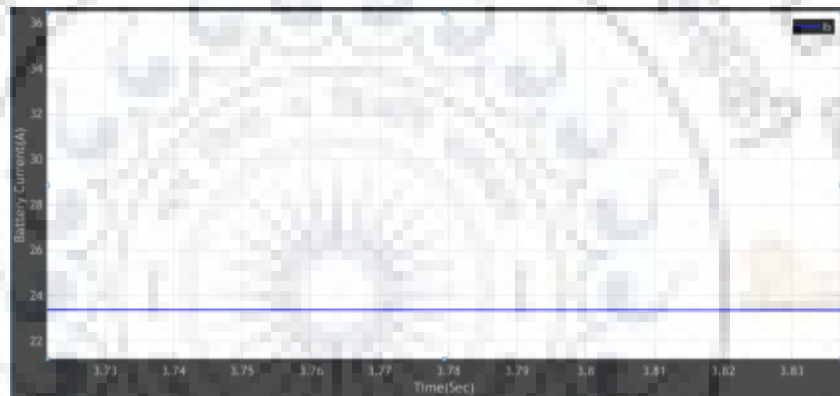

Fig.4. 13 DC-link Voltage

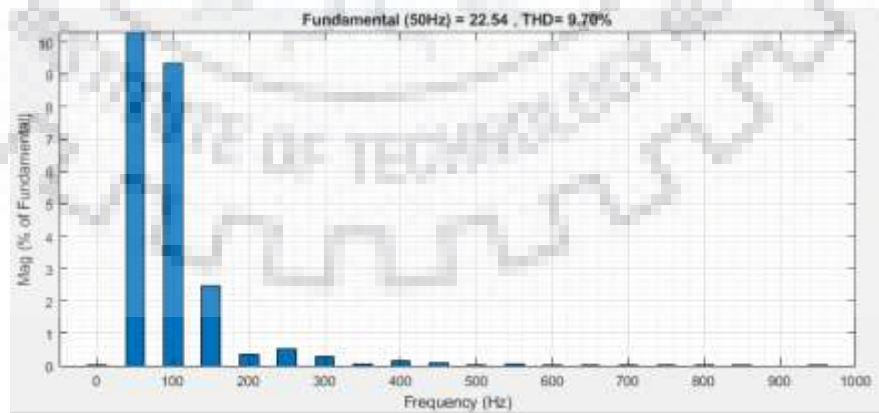Fig.4. 14 Battery Voltage

Fig.4. 15 Battery Current (Ib)

Fig.4. 16 FFT analysis of Grid Current

37

CONCLUSION

In the first part the modelling and simulation of bi-directional battery charger for an electric vehicle with a capability to exchange both active and reactive powers with the grid simultaneously have been presented in detail. The system is simulated in Matlab/Simulink and the control algorithm for proposed charger with operating modes has been verified. Similarly in the second part of discussion the performance of proposed single stage solar PV array based bi-directional EV charger has been presented under both active and reactive power flows. Test results have verified that along with performing its primary tasks of charging the EV battery, the proposed charger has integrated the solar PV array very efficiently. Moreover, the elimination of DC-DC boost converter has not affected the performance of the solar PV array, and VSC has performed the task of harnessing the maximum power from the solar PV array. The various SteadyState results have proved the promptness of the controller, capability to maintain the sinusoidal grid voltage and current and power quality of the grid voltage and current within the IEEE 519 standard.

APPENDIX

---

1.   Specification Used in Concerned Research Paper

Battery Specifications: 300V, 500Ah li-ion battery Converter specification:

Parameters	Symbol	Value
AC side filter capacitor	C_{ac}	330μF
Coupling inductance	L_c	5mH
DC link capacitor	C_{DC}	2000μF
DC side filter inductor	C_{ac}	5mH
DC side filter capacitor	C_b	700μF
DC link voltage	V_{DC}	400V

2.   Specification Used in Case Study and Simulation

Battery Specifications: 415V, 500Ah li-ion battery Converter specification:

Parameters	Symbol	Value
AC side filter capacitor and resistance	C_{ac}, R_{ac}	330μF,1 ohm
Coupling inductance	L_c	27mH
DC link capacitor	C_{DC}	5000μF

DC side filter inductor and resistance	L_b, R_b	3mH, 2.5ohm
DC side filter capacitor	C_b	700µF
DC link voltage	V_{DC}	400V
Source side inductance	L_S	7mH

3. Matlab program for MPPT Control using Perturb and Observe Technique

```matlab
function D  = PandO(Param, Enabled, V, I)

% MPPT controller based on the Perturb & Observe algorithm.

% D output = Reference for DC link voltage (Vdc_ref)
%
% Enabled input = 1 to enable the MPPT controller
% V input = PV array terminal voltage (V)
% I input = PV array current (A)
%
% Param input:
Dinit = Param(1);  %Initial value for Vdc_ref
Dmax = Param(2);   %Maximum value for Vdc_ref
Dmin = Param(3);   %Minimum value for Vdc_ref
deltaD = Param(4); %Increment value used to increase/decrease Vdc_ref
%

persistent Vold Pold Dold;

dataType = 'double';

if isempty(Vold)
   Vold=0;
   Pold=0;
   Dold=Dinit;
end
P= V*I;
dV= V - Vold;
dP= P - Pold;

if dP ~= 0 & Enabled ~=0
```
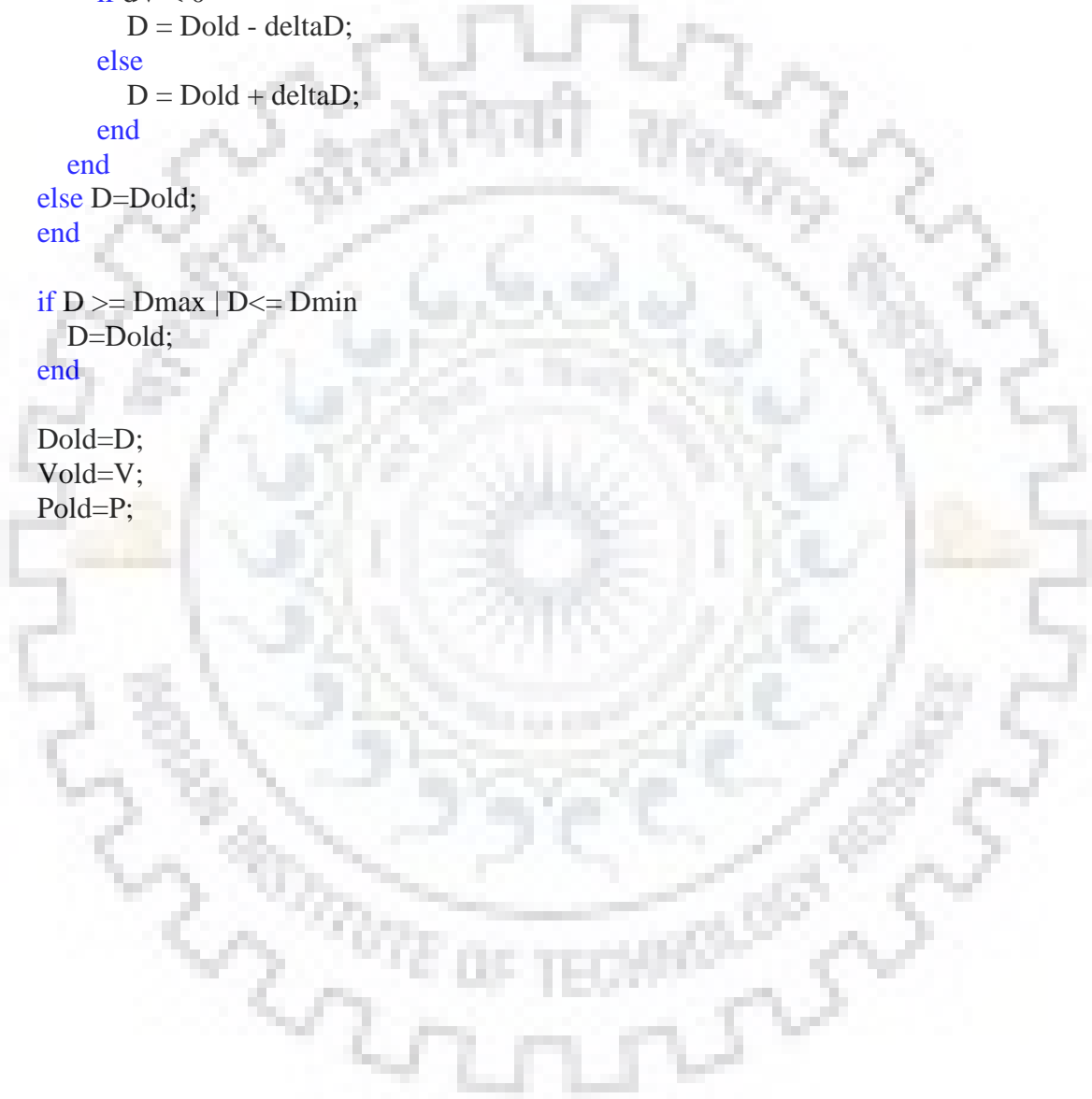
40

```
    if dP < 0
      if dV < 0
         D = Dold + deltaD;
      else
         D = Dold - deltaD;
      end
    else
      if dV < 0
         D = Dold - deltaD;
      else
         D = Dold + deltaD;
      end
    end
else D=Dold;
end

if D >= Dmax | D<= Dmin
   D=Dold;
end

Dold=D;
Vold=V;
Pold=P;
```

REFERENCES

[1]   M. Restrepo, S. Member, J. Morris, M. Kazerani, S. Member, and C. A. Cañizares, "Modeling and Testing of a Bidirectional Smart Charger for Distribution System EV Integration," *IEEE Trans. Smart Grid*, vol. 9, no. 1, pp. 152–162, 2018.

[2]   B. Shingh and A. Verma, "An Implementation of Solar PV Array Based Multifunctional EV Charger," *2018 IEEE Transp. Electrif. Conf. Expo*, pp. 531–536, 2018.

[3]   R. J. Aguero, E. Takayesu, and R. Masiello, "Modernizing the Grid: Challenges and Opportunities for a Sustainable Future," *IEEE Power Energy Mag.*, vol. 15, no. April, pp. 74–83, 2017.

[4]   H. N. De Melo *et al.*, "A Controllable Bidirectional Battery Charger for Electric Vehicles with Vehicle-to-Grid Capability," *IEEE Trans. Veh. Technol.*, vol. 67, no. 1, pp. 114–123, 2018.

[5]   M. O. Badawy, Y. Sozer, and S. Member, "Power Flow Management of a Grid Tied PV-Battery System for Electric Vehicles Charging," *IEEE Trans. Ind. Appl.*, vol. 53, no. 2, pp. 1347–1357, 2017.

[6]   V. Monteiro, S. Member, J. G. Pinto, S. Member, and J. L. Afonso, "Operation Modes for the Electric Vehicle in Smart Grids and Smart Homes : Present and Proposed Modes," *IEEE Trans. Veh. Technol.*, vol. 65, no. 3, pp. 1007–1020, 2016.

[7]   F. Berthold, A. Ravey, B. Blunier, D. Bouquain, S. Williamson, and S. Member, "Design and Development of a Smart Control Strategy for Plug-In Hybrid Vehicles Including Vehicle-to-Home Functionality," *IEEE Trans. Transp. Electrif.*, vol. 1, no. 2, pp. 168–177, 2015.

[8]   R. Kumar and S. Member, "Buck-Boost Converter Fed BLDC Motor Drive for Solar PV Array Based Water Pumping," *2014 IEEE Int. Conf. Power Electron. Drives Energy Syst.*, pp. 1–6, 2014.

[9]   M. Brenna, F. Foiadelli, and M. Longo, "The Exploitation of Vehicle-to-Grid Function for Power Quality Improvement in a Smart Grid," *IEEE Trans. Intell. Transp. Syst.*, vol. 15, no. 5, pp. 2169–2177, 2014.

[10]   F. Marra *et al.*, "EV Charging Facilities and Their Application in LV Feeders With Photovoltaics," *IEEE Trans. Smart Grid*, vol. 4, no. 3, pp. 1533–1540, 2013.

[11]   S. J. Gunter, S. Member, K. K. Afridi, and D. J. Perreault, "Optimal Design of Grid-Connected PEV Charging Systems With Integrated Distributed Resources," *IEEE Trans. Smart Grid*, vol. 4, no. 2, pp. 956–967, 2013.

[12]   B. D. Bowermaster and M. Alexander, "The Need for Charging," *IEEE Electrif. Mag.*, vol. 5, no. March 2017, pp. 59–67, 2011.